Review

Nondestructive measurement of fruit and vegetable quality by means of NIR spectroscopy: A review

Bart M. Nicolaï [a,*], Katrien Beullens [a], Els Bobelyn [a], Ann Peirs [a],
Wouter Saeys [a], Karen I. Theron [b], Jeroen Lammertyn [a]

[a] *Flanders Centre of Postharvest Technology/BIOSYST-MeBioS, Catholic University of Leuven, Willem de Croylaan 42, 3001 Leuven, Belgium*
[b] *Department of Horticultural Science, University of Stellenbosch, Private Bag X1, Matieland 7602, South Africa*

Abstract

An overview is given of near infrared (NIR) spectroscopy for use in measuring quality attributes of horticultural produce. Different spectrophotometer designs and measurement principles are compared, and novel techniques, such as time and spatially resolved spectroscopy for the estimation of light absorption and scattering properties of vegetable tissue, as well as NIR multi- and hyperspectral imaging techniques are reviewed. Special attention is paid to recent developments in portable systems. Chemometrics is an essential part of NIR spectroscopy, and the available preprocessing and regression techniques, including nonlinear ones, such as kernel-based methods, are discussed. Robustness issues due to orchard and species effects and fluctuating temperatures are addressed. The problem of calibration transfer from one spectrophotometer to another is introduced, as well as techniques for calibration transfer. Most applications of NIR spectroscopy have focussed on the nondestructive measurement of soluble solids content of fruit where typically a root mean square error of prediction of 1° Brix can be achieved, but also other applications involving texture, dry matter, acidity or disorders of fruit and vegetables have been reported. Areas where more research is required are identified.
© 2007 Elsevier B.V. All rights reserved.

Keywords: NIR; Near infrared; Fruit; Reflectance; Interactance; Transmittance; Chemometrics; PLS; Nondestructive; Quality

Contents

* Corresponding author. Tel.: +32 16 322375; fax: +32 16 322955.
 E-mail address: bart.nicolai@biw.kuleuven.be (B.M. Nicolaï).

1. Introduction

Near infrared (NIR) radiation covers the range of the electromagnetic spectrum between 780 and 2500 nm. In NIR spectroscopy, the product is irradiated with NIR radiation, and the reflected or transmitted radiation is measured. While the radiation penetrates the product, its spectral characteristics change through wavelength dependent scattering and absorption processes. This change depends on the chemical composition of the product, as well as on its light scattering properties which are related to the microstructure. Advanced multivariate statistical techniques, such as partial least squares regression are then applied to extract the required information from the usually convoluted spectra.

NIR spectroscopy was first used in agricultural applications by Norris (1964) to measure moisture in grain. Since then it has been used for rapid analysis of mainly moisture, protein and fat content of a wide variety of agricultural and food products (Davies and Grant, 1987; Gunasekaran and Irudayaraj, 2001). Early applications in horticulture focussed on dry matter content of onions (Birth et al., 1985), soluble solids content (SSC) of apples (Bellon-Maurel, 1992) and water content of mushrooms (Roy et al., 1993), but since then many other applications have followed. As the propagation of NIR radiation in fruit and vegetable tissue is affected by their microstructure, it was soon discovered that NIR spectroscopy could also be used to measure microstructure-related attributes, such as stiffness (Lammertyn et al., 1998), internal damage (Clark et al., 2003a,b), and even sensory attributes (Mehinagic et al., 2004). Recent developments which extend the potential of NIR spectroscopy further include multi- and hyperspectral imaging techniques which also provide spatial information (Martinsen and Schaare, 1998; Lu, 2003) and time-resolved spectroscopy which allows measurement of absorption and scattering processes separately (Cubeddu et al., 2001).

The increasing importance of NIR spectroscopy in postharvest technology is obvious from the recent increase in numbers of publications, as well as from the fact that many manufacturers of on-line grading lines have now implemented NIR systems to measure various quality attributes. The objective of this review is to give a comprehensive overview of NIR spectroscopy for measuring quality attributes of fruit and vegetables. We will pay attention to optics and chemometrics as well as applications, and will try to identify areas where more research is required.

2. Principles and instrumentation

2.1. Basic concepts of near infrared spectroscopy

Near infrared radiation was discovered by Friedrich Wilhelm Herschel in 1800 (Davies, 2000) and covers by definition the wavelength range from 780 to 2500 nm. When radiation hits a sample, the incident radiation may be reflected, absorbed or transmitted, and the relative contribution of each phenomenon depends on the chemical constitution and physical parameters of the sample.

Reflection is due to three different phenomena. Specular reflection causes gloss, whereas external diffuse reflection is induced by rough surfaces. Both only provide information about the surface of the sample. Scattering results from multiple refractions at phase changes inside the material. The main scattering elements in fruit and vegetables are the cell wall interfaces since they induce abrupt changes in refractive index (McGlone et al., 1997), but suspended particles, such as starch granules, chloroplasts and mitochondria may also induce scattering caused by diffraction at the particle surface where the refractive index is different from that of the surroundings (Il'yasov and Krasnikov, 1991). The scattering is also dependent on the size, the shape and microstructure of the particles. Scattering may also appear due to heterogeneities, such as pores, openings, capillaries that are randomly distributed through the sample. Multiple scattering events largely determine the intensity of the scattered light that is emitted (McGlone et al., 1997). The scattering process affects the intensity level of the reflected spectrum rather than the shape; the latter is more related to the absorption process.

Most absorption bands in the near infrared region are overtone or combination bands of the fundamental absorption bands in the infrared region of the electromagnetic spectrum which are due to vibrational and rotational transitions. In large molecules and in complex mixtures, such as foods, the multiple bands and the effect of peak-broadening result in NIR spectra that have a broad envelope with few sharp peaks. In Fig. 1, typical NIR reflectance spectra of some fruit are shown (see also Sharpe and Barber, 1972 for other typical spectra). The spectra are clearly very similar and are dominated by the water spectrum with overtone bands of the OH-bonds at 760, 970 and 1450 nm and a combination band at 1940 nm (Polessello and Giangiacomo, 1981). This similarity is the reason why sophisticated multivariate statistical
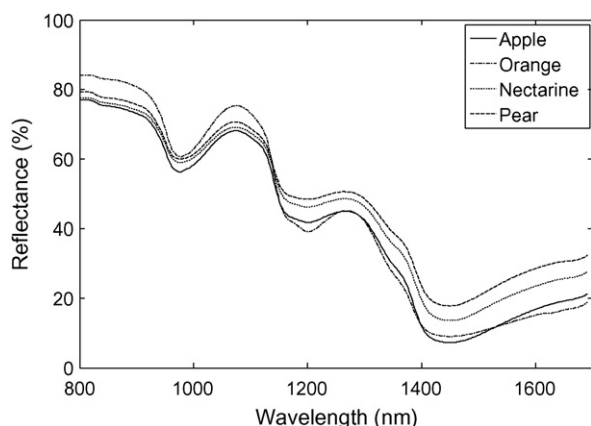
Fig. 1. Typical NIR reflectance spectra of some fruit. The NIR reflectance spectra were recorded using a Corona 45 Vis/NIR diode array spectrophotometer (Carl Zeiss Jena Gmbh, Jena, Germany) as described in Nicolaï et al. (2006a).

techniques are essential to extract useful information from an NIR spectrum.

2.2. Equipment

2.2.1. Spectrophotometers

An NIR spectrophotometer consists of a light source (usually a tungsten halogen light bulb), sample presentation accessory, monochromator, detector, and optical components, such as lenses, collimators, beam splitters, integrating spheres and optical fibers. Spectrophotometers are conveniently classified according to the type of monochromator. In a *filter* instrument, the monochromator is a wheel holding a number of absorption or interference filters. Its spectral resolution is limited. In a *scanning monochromator* instrument a grating or a prism is used to separate the individual frequencies of the radiation either entering or leaving the sample. The wavelength separator rotates so that the radiation of the individual wavelengths subsequently reaches the detector. *Fourier transform* spectrophotometers use an interferometer to generate modulated light; the time domain signal of the light reflected or transmitted by the sample onto the sample can be converted into a spectrum via a fast Fourier transform. Often a Michelson interferometer is used, but also polarisation interferometers are used in some spectrophotometers. In *photodiode array* (PDA) spectrophotometers, a fixed grating focuses the dispersed radiation onto an array of silicon (350–1100 nm) or InGaAs (Indium Gallium Arsenide, 1100–2500 nm) photodiode detectors. *Laser* based systems do not contain a monochromator but have different laser light sources or a tunable laser. *Acoustic optic tunable filter* (AOTF) instruments use a diffraction based optical-band-pass filter that can be rapidly tuned to pass various wavelengths of light by varying the frequency of an acoustic wave propagating through an anisotropic crystal medium. Finally, *liquid crystal tunable filter* (LCTF) instruments use a birefringent filter to create constructive and destructive interference based on the retardation, in phase between the ordinary and extraordinary light rays passing through a liquid crystal. In this way they act as an interference filter to pass a single wavelength of light. By combining several

electronically tunable stages in series, high spectral resolution can be achieved (Stratis et al., 2001).

There is definitely a shift towards PDA systems because their high acquisition speed (the integration time is typically 50 ms but can be as low as a few milliseconds) and the absence of moving parts enables them to be mounted on online fruit grading lines. Miniaturised versions are available from companies, such as Ocean Optics (Dunedin, FL, USA), Zeiss (Jena, Germany), Oriel (Stratford, CT, USA), and Integrated Spectronics (Baulkham Hills, Australia). Guidelines for selecting an appropriate spectrophotometer are given by Walsh et al. (2000).

Optical instruments should be handled with care. Manipulation may break optical fibers and decrease the signal to noise ratio. Excessive bending of a fiber optic cable may affect its spectral response. Dust is to be avoided by all means, and it is important to keep the white reference clean for obvious reasons. The light source should be switched on well in advance because the spectral characteristics change during the warming up period. The integration time for PDA detectors should ideally be sufficient to obtain a detector response of about 50% of saturation.

2.2.2. Measurement setup

Three different measurement setups for obtaining near infrared spectra are shown in Fig. 2. In reflectance mode (Fig. 2a), light source and detector are mounted under a specific angle, e.g., 45°, to avoid specular reflection. In transmittance mode the light source is positioned opposite to the detector, while in interactance mode the light source and detector are positioned parallel to each other in such a way that light due to specular reflection cannot directly enter the detector. This can be achieved by means of a bifurcated cable in which fibers leading to the source and detector are parallel to each other and in contact with the product, or by means of a special optical arrangement (e.g., Greensill and Walsh, 2000a; McGlone et al.,
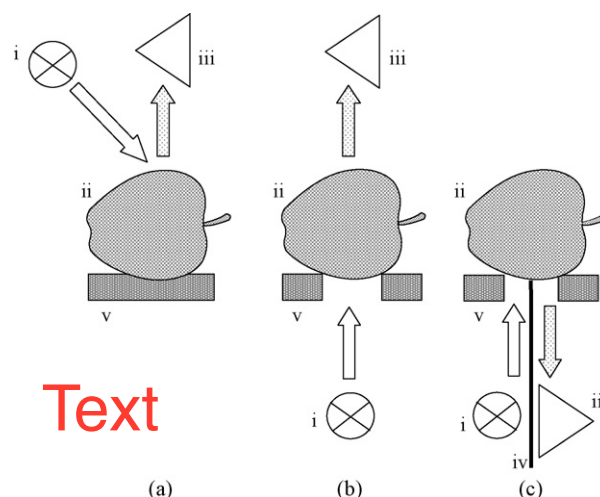

Fig. 2. Setup for the acquisition of (a) reflectance, (b) transmittance, and (c) interactance spectra, with (i) the light source, (ii) fruit, (iii) monochromator/detector, (iv) light barrier, and (v) support. In interactance mode, light due to specular reflection is physically prevented from entering the monochromator by means of a light barrier.

2002a). In both reflectance and transmittance mode integrated spheres may also be used to collect light and increase the signal to noise ratio.

In selecting the measurement setup, it is important to know that the penetration of NIR radiation into fruit tissue decreases exponentially with the depth (Lammertyn et al., 2000; Fraser et al., 2000; Greensill and Walsh, 2000a). Lammertyn et al. (2000) found a penetration depth of up to 4 mm in the 700–900 nm range and between 2 and 3 mm in the 900–1900 nm range for apple. They defined the light penetration depth as the slice thickness for which the diffuse reflectance spectra were significantly different from those of a slice of infinite thickness. In a different optical configuration, Fraser et al. (2000) showed that the penetration depth (defined as the depth at which the light intensity dropped to 1% of the initial intensity) in apple in the 700–900 nm range was at least 25 mm, while it became less than 1 mm in the 1400–1600 nm range. Further, they found based on both measurements as well as Monte Carlo simulations into mandarin fruit that the skin poses a major barrier for light penetration, even at 808 nm (Fraser et al., 2003). This may also explain the relatively poor predictions of SSC in grapefruit which were obtained by Miller and Zude-Sasse (2004). The limited penetration depth restricts the potential of reflectance or interactance measurements for detecting internal defects, and decreases the accuracy of NIR based measurements of internal quality attributes of thick-skinned fruit, such as citrus. Transmission measurements, on the other hand, need very high light intensities which can easily burn the fruit surface and alter its spectral properties. Also, the transmitted light carries information about the skin and the core of the fruit which might or might not be relevant, depending on the application.

In biomedical optics an increased understanding of the light penetration into mammalian tissue has been obtained by means of numerical solution of the light transport equation. Several approaches have been followed including the diffusion approximation (Farrell and Patterson, 1992), adding-doubling (Prahl, 1995) and the Monte Carlo method (Wang et al., 1995; Jacques, 1998). More research involving these types of numerical simulation techniques is required to improve our understanding of light penetration in fruit tissue.

Schaare and Fraser (2000) compared reflectance, interactance and transmission measurements to measure SSC, density and internal flesh colour of yellow-fleshed kiwifruit. They found that interactance mode spectra provided the most accurate estimates. Lammertyn et al. (2000) found only marginal differences between reflectance and interactance measurements to determine SSC of apple.

2.2.3. Multi- and hyperspectral imaging systems

Most applications of NIR spectroscopy which are described in the literature essentially rely on spot measurements. However, Peiris et al. (1999) observed a circumferential variation of up to 2% Brix for the SSC in a variety of fruit; the radial and proximal to distal variation was even larger. Martinsen and Schaare (1998) found similar results for the distribution of the SSC in kiwifruit cross-sections. Sugiyama (1999) found spatial differences from 5 to 10% Brix in cross-sections of unripe and ripe

melons, respectively. Likewise, Long and Walsh (2006) showed that the SSC of the outer mesocarp of melon was 3° Brix higher at the stylar end of the fruit compared with the stem end. Also, the SSC of the inner mesocarp was higher than that of the outer tissue and more uniform across spatial positions.

Depending on the uniformity of the quality attribute within the fruit, it might be necessary to repeat the spectral acquisition at several positions on the fruit or vegetable. This is insufficient when, for example, skin disorders are to be detected in a practical application; the whole surface of the fruit then must be inspected. In this case multispectral (a few wavelengths) or hyperspectral (a continuous range of wavelengths) imaging systems are required. Such systems produce a spectral data cube—a spectrum at every 2D spatial position.

In early systems (e.g., Upchurch and Throop, 1994) a sequence of spatial images was acquired by means of an NIR camera and a set of band-pass filters. While the acquisition can be fast, the disadvantage of this approach is that only a limited number of wavelengths can be analysed and that they need to be known a priori. In a more recent approach (e.g., Martinsen and Schaare, 1998) a line of spatial information with a full spectral range per spatial pixel is captured sequentially to complete a volume of spatial-spectral data. This is usually achieved by means of a spectrograph which disperses an incoming line of radiation into a spectral and spatial matrix which is captured by the camera. The horizontal and vertical pixels on the camera capture spatial and spectral information, respectively. Such a system, hence, provides full spectral information at every spatial position. The object must be moved stepwise under the camera by means of an actuactor while at each step a line is scanned, but is not necessarily a disadvantage when the system is mounted on a grading line on which the fruit is physically transported anyway. Novel developments include focal plane array cameras in combination with liquid crystal tunable filters (LCTF), acousto-optical tunable filters (AOTF) or other monochromator principles which allow for much faster acquisition speeds (Bearman and Levenson, 2001). Examples of multi- and hyperspectral imaging will be discussed later.

2.2.4. Spatially and time-resolved spectroscopy

As mentioned before, a typical reflectance or transmittance spectrum of fruit contains information on both absorption as well as scattering. While absorption is related to the presence of chemical components, scattering is related to the microstructure of the tissue. As the microstructure of tissue is related to macroscopic texture properties of the fruit (Oey et al., 2007), several authors have attempted to develop techniques to measure absorption and scattering properties separately. McGlone et al. (1997) measured the intensity of scattered laser light at 864 nm in kiwifruit exiting the fruit at various angles between 20° and 55°. They found an R^2 of 72 and 67% for regression of the scattered light intensity against stiffness and rupture force. Tu et al. (1995, 2000) projected a He–Ne laser light beam on the surface of a tomato and used a CCD camera to measure the area of the spot as an indication of the amount of scattering and, hence, fruit firmness. De Belie et al. (1999) used the same technique to measure changes of apples during shelf-life exposure,

and found an increase in spot size which was, however, not correlated with changes in turgor pressure, which is proportional to fruit stiffness (Oey et al., 2007). Lu (2004a,b) extended this method by using broadband light in the range 688–940 nm, and analysed the scattering profiles by means of a backpropagation neural network. He obtained a standard error of prediction (SEP) of about 6 N for Magness Taylor firmness and 0.78% Brix for the soluble solids content (SSC) of apples. As these methods rely on spatial information, they can be classified as space resolved reflectance spectroscopy.

A completely different approach was followed by Cubeddu et al. (2001) who used time domain reflectance spectroscopy (TRS) to measure quality attributes of fruit. Series of very short (pico or femto second) NIR light pulses are pumped into the fruit using a tunable laser or a solid-state laser array. The detector is positioned at some distance from the light entry point. Depending on the scattering properties of the tissue, the photons may follow a complicated path in the tissue and it may take more or less time to reach the detector. As a result, the detector will measure a photon time of flight distribution from which based on light diffusion theory the absorption and scattering coefficient as a function of wavelength can be measured. These coefficient spectra can then be correlated to internal quality attributes. By comparing classical NIR reflectance measurements of pear with the corresponding absorption and scattering coefficient spectra obtained through TRS, Nicolaï et al. (2007) showed that NIR reflectance is dominated by scattering which does not change much with wavelength. While TRS is certainly an exciting development, the equipment is complicated, and so far the obtained correlations between absorption and scattering spectra and quality attributes, such as SSC or firmness were low (Valero et al., 2004) to non-existent (Nicolaï et al., 2007), most probably due to instrument drift or the limited wavelength range ($\leq$1030 nm) considered in the experiments. It is also important to note that light diffusion in fruit is affected by both absorption and reflection properties of the tissue simultaneously, and it is not possible to measure them independently.

2.2.5. Portable spectrophotometers

The availability of low cost miniaturised spectrophotometers has opened up the possibility of portable devices which can be used in the orchard for monitoring the maturity of fruit. Obviously, the interference of the environment, such as ambient light and fluctuating temperatures should be either minimised or accounted for by appropriate data processing (see Sections 3.6 and 3.8). Ventura et al. (1998) used a miniature spectrometer with a range of 350–999 nm to measure the SSC of apple fruit. They constructed a box with a special rubber ring for positioning the fruit to minimise environmental stray light interference and obtained a root mean square error of prediction (RMSEP) of 1.1% Brix. Walsh et al. (2000) compared the performance characteristics of three low cost commercial miniature spectrometers to measure SSC of rockmelons and found clear differences in spectral resolution and stability, relative detector sensitivity, signal to noise ratio, stability over time and variability in temperature and calibration performance. A European consortium of research institutes constructed a portable glove-shaped

apparatus which was equipped with various miniaturised sensors for measuring SSC, mechanical properties, internal colour and maturity (Hernández Sánchez et al., 2003) for use during picking. The SSC was measured by means of a miniaturised Vis/NIR spectrometer mounted on the glove. Other applications of portable devices have been described by Temma et al. (2002a), Saranwong et al. (2003a,b), Miller and Zude-Sasse (2004), and Zude et al. (2006). All portable devices which have been described so far used silicon diode arrays as they are much cheaper than InGaAs arrays. However, in all cases except one in which the commercially available FANTEC Fruit Tester 20 was used (Saranwong et al., 2003a), relatively poor prediction accuracy was obtained. This might be due to robustness issues, such as temperature fluctuations, the limited silicon wavelength range, or the fact that the devices were self made prototypes and not laboratory grade spectrophotometers. As there is certainly a large scope for applications of portable devices, more research is required in this area.

3. Chemometrics

Water is the most important chemical constituent of most fruit and vegetables. As water highly absorbs near infrared radiation, the near infrared spectrum of fruit and vegetables is dominated by water. Further, the near infrared spectrum is essentially composed of a large set of overtones and combination bands. This, in combination with the complex chemical composition of a typical fruit or vegetable causes the near infrared spectrum to be highly convoluted. Finally, the spectrum may further be complicated by wavelength dependent scattering effects, tissue heterogeneities, instrumental noise, ambient effects and other sources of variability. As a consequence, it is difficult to assign specific absorption bands to specific functional groups let alone chemical components. Multivariate statistical techniques (also called chemometrics) are therefore required to extract the information about quality attributes which is buried in the NIR spectrum ('model calibration'). Essentially this involves regression techniques coupled with spectral preprocessing (Geladi and Dåbakk, 1995). As most applications in the literature involve regression rather than classification, we will not discuss techniques for the latter here. An overview of linear and nonlinear techniques for classification of fruit based on Vis/NIR spectra can be found in Kim et al. (2000).

3.1. Spectral preprocessing techniques

Spectral preprocessing techniques are used to remove any irrelevant information which cannot be handled properly by the regression techniques. Several preprocessing methods have been developed for this purpose and the reader is referred to the literature for further details (Martens and Næs, 1998; Næs et al., 2004).

3.1.1. Averaging

Averaging over spectra is usually carried out during the acquisition of the spectrum to reduce the thermal noise of the

detector. The number of scans depends on the application: in online grading systems PDA spectrophotometers operate at a typical acquisition time below 50 ms, and little time is available for acquiring more than one scan; in the laboratory, PDA spectrophotometer measurement time is less critical and several spectra can be averaged without affecting the measurement throughput rate. The required number obviously depends on its signal to noise ratio of the spectrophotometer. Greensill and Walsh (2000b) found that the optimal signal to noise ratio for calibrations of sucrose in a water–cellulose matrix was 5000:1. To evaluate the effect of noise on calibration model performance, Nicolaï et al. (2006a) added Gaussian noise with a standard deviation of 0.1% to (10 times inflated) reflectance spectra of apple. They did not find any effect after wavelength compression and denoising. This suggests that a signal to noise ratio of 1000:1 is sufficient. More research is required.

Averaging over wavelengths is used to reduce the number of wavelengths or to smooth the spectrum. Modern spectrophotometers typically have an optical resolution beyond 10 nm, whereas a 10 nm resolution is often sufficient for most applications. Also, most spectrophotometers provide a better spectral resolution (often 1–2 nm) than the actual optical resolution; while this certainly increases statistical processing time it does not improve the information content of the spectra. Further, below 1100 nm the bandwidth of absorption peaks is typically larger than 40 nm (Greensill et al., 2001, and references therein). Nicolaï et al. (2006a) artificially inflated NIR reflectance spectra of apple with a 2 nm resolution tenfold to 0.2 nm resolution; artificial reflectance values between two neighbouring wavelengths in the original spectra were obtained by linear interpolation, and Gaussian noise was added. The accuracy of the corresponding PLS model was very low but increased by removing redundant high resolution information by means of wavelet compression. The best results were obtained with compression ratios of 20–30, loosely corresponding to a wavelength resolution of about 5 nm.

3.1.2. Centering

The first stage in pre-processing is often to subtract the average from each variable. This operation is called mean centering and ensures that all results will be interpretable in terms of variation around the mean. It is recommended for all practical applications.

3.1.3. Smoothing

Several smoothing techniques have been proposed to remove random noise from near infrared spectra, including moving average filters and the Savitzky–Golay algorithm (Næs et al., 2004). While smoothing obviously improves the visual aspect of the near infrared spectra, it does remove information at a stage where it is not clear yet whether this information is useful. As the multivariate regression techniques which are typically used after preprocessing already incorporate an explicit model for additive noise (Næs et al., 2004), there does not seem to be a good reason to smooth near infrared spectra.

3.1.4. Standardisation

Standardisation means dividing the spectrum at every wavelength by the standard deviation of the spectrum at this wavelength. Typically variances of all wavelengths are standardised to 1, which results in an equal influence of the variables in the model, but other standardisation procedures are possible as well (Næs et al., 2004). While standardisation is commonly used when variables are measured in different units or have different ranges, it is to be avoided in NIR spectroscopy since the noise on a variable with a small standard deviation can blow up, and, therefore, can result in a less reliable model.

3.1.5. Normalisation

While most chemometrics software packages offer several normalisation methods, multiple scatter correction (MSC) is the most popular normalisation technique (Næs et al., 2004). It is used to compensate for additive (baseline shift) and multiplicative (tilt) effects in the spectral data, which are induced by physical effects, such as the non-uniform scattering throughout the spectrum as the degree of scattering is dependent on the wavelength of the radiation, the particle size and the refractive index. The method attempts to remove the effects of scattering by linearising each spectrum to some 'ideal' spectrum of the sample, which, in practice, corresponds to the average spectrum. Extended multiple scatter correction (EMSC) is an extension of MSC and allows to compensate also for chemical interference effects by incorporating known spectra of the interferents and analytes (Martens and Stark, 1991). The value of EMSC in applications of NIR spectroscopy to fruit and vegetables still needs to be exploited. In standard normal variate correction (SNV), each individual spectrum is normalised to zero mean and unit variance.

3.1.6. Transformation

Derivation is used often to remove baseline shifts and superposed peaks. Derivative spectra of order two are most popular as they can correct for both additive and multiplicative effects (like MSC). They are usually calculated according to the Savitzky–Golay algorithm (Næs et al., 2004). The choice between MSC and the Savitzky–Golay algorithm is a matter of taste. The parameters of the algorithm (interval width, polynomial order) should be selected carefully in order to avoid amplification of spectral noise. Note that these parameters should not be considered as tuning parameters.

Spectroscopic measurements performed in transmission mode can be quantified using Beer's Law (concentration $\sim \log(1/T)$ where T is the transmitted radiation). Accordingly, reflectance measurements are frequently converted to $\log(1/R)$, which are then used in a similar way to optical density readings. This approach ignores the fact that light penetration in biological tissue is much more complicated and also involves scattering (Davies and Grant, 1987). The Kubelka–Munck transformation $(1–R^2)/2R$ does account for scattering, but for diffuse reflection measurements of agricultural products $\log(1/R)$ has been shown to be preferable (Griffiths, 1995). Overall, there does not seem to be a large advantage of either transformation method compared to the untransformed spectra (Nicolaï et al., 2006a).

3.2. Linear regression techniques

Multivariate regression techniques aim at establishing a relationship between the $n \times 1$ vector of observed response values **y** ('Y-variables'; quality attributes of interest, such as soluble solids content and firmness) and the $n \times N$ spectral matrix **X** ('X-variables'), with n the number of spectra and N the number of wavelengths.

In *multiple linear regression* (MLR) **y** is approximated by a linear combination of the spectral values at every single wavelength. The N regression coefficients are estimated by minimising the error between predicted and observed response values in a least squares sense. A stepwise multiple linear regression (SMLR) technique may be applied to select a number of variables for the equation. SMLR selects first the variable with the largest correlation with the Y-data, then a second variable that results in the best improvement of the accuracy of the prediction, then a third variable and so on until no further significant improvement can be obtained. MLR models typically do not perform well because of the often high co-linearity of the spectra and easily lead to overfitting and loss of robustness of the calibration models (Næs et al., 2004).

Principal component regression is a two-step procedure, which first decomposes the **X** by a principal component analysis (PCA) and then fits a MLR model, using a small number of principal components (PCs) (or latent variables) instead of the original variables as predictors. The advantage with respect to MLR is that the X-variables (PCs) are uncorrelated, and that the noise is filtered. Also, usually a small number of PCs is sufficient. A drawback is that the principal components are ordered according to decreasing explained variance of the spectral matrix, and that the first principal components which are used for the regression model are not necessarily the most informative with respect to the response variable (Wold et al., 2001).

Partial least squares regression (PLS) was introduced almost 30 years ago by Wold to overcome this disadvantage (Wold et al., 2001, and references therein). In PLS regression an orthogonal basis of latent variables is constructed one by one in such a way that they are oriented along directions of maximal covariance between the spectral matrix **X** and the response vector **y**. In this way it is ensured that the latent variables are ordered according to their relevance for predicting the Y-variable. Interpretation of the relationship between X-data and Y-data (the regression model) is then simplified as this relationship is concentrated on the smallest possible number of latent variables. The method performs particularly well when the various X-variables express common information, i.e., when there is a large amount of correlation, or even co-linearity, which is the case for spectral data of intact biological material. The required number of latent variables is typically smaller than that in a PCR calibration model for a similar model performance. PLS regression can be easily extended to simultaneously predict several quality attributes. In this case the algorithm is called PLS2 (Næs et al., 2004).

Several software packages are available for multivariate calibration. The Unscrambler package (http://www.camo.com) is menu-driven, very easy to use and offers a range of preprocessing techniques. The Grams Suite is a general purpose software package for handling spectroscopic data including chemometrics and is distributed by the Thermo Scientific company (http://www.thermo.com). The Matlab PLS toolbox of Eigenvector Research (software.eigenvector.com) offers the flexibility of Matlab for applications in which programming is required. Many statistical packages, such as SAS (http://www.sas.com) and statistica (http://www.statsoft.com) also provide multivariate calibration but are less convenient to use for processing spectral data.

3.3. Nonlinear regression techniques

Y-Residual plots show the residuals (predicted minus measured Y-variables) versus the predicted Y-variables. A curvilinear trend in these plots may indicated nonlinearities. In this case it might be useful to use nonlinear regression techniques. However, the Y-residual plots do not always allow detection of nonlinearities. Depending on the structure of the original dataset the PLS model may automatically select linear features; possible nonlinear features may then appear in the residuals plot as random noise rather than a curvilinear trend. An example of such hidden nonlinearities has been described by Isaksson and Næs (1988).

Artificial neural networks (ANN) have been used to construct NIR calibration models (Næs et al., 1993; Geladi et al., 1996). The most widely used ANN is the so-called multilayer perceptron (MLP) which typically consist of three layers of so-called neurons, the input, hidden, and output layer. Every neuron of the input layer is connected to every neuron of the hidden layer, and every neuron of the hidden layer is connected to every neuron of the output layer. A neuron is a computational device that calculates the weighted sum of its inputs and calculates the output signal from this using a nonlinear function. The spectral value at every wavelength is fed to the input layer, while the output layer delivers the prediction of the attribute. The weights are estimated using an appropriate algorithm based on a calibration set using cross validation (Kim et al., 2000). Most applications of ANNs in postharvest technology have been for classification purposes (Guyer and Yang, 2000; Kim et al., 2000; Hahn et al., 2004). Næs et al. (1993) concluded that even though ANNs may in certain cases be better than linear techniques, they are more difficult to understand and the results are more difficult to visualise and interpret.

Kernel-based techniques are becoming more popular because, in contrast to ANNs, they allow interpretation of the calibration model. In kernel-based methods the calibration is carried out in a space of nonlinearly transformed input data – the so-called feature space – without actually carrying out the transformation. The feature space is defined by the so-called kernel function, a measure of similarity between two spectra. The most popular kernel functions are the Gaussian and polynomial functions (Nicolaï et al., 2006a). Kernel versions of the PCR and PLS algorithms have been described in literature (Rosipal and Trejo, 2001; Shawe-Taylor and Cristianini, 2004). Least squares support vector machines (LS-SVM) is essentially a kernel-based multiple regression procedure which incorporates a second tuning parameter – the so-called regularisation parameter Γ – which

penalises large values of the regression coefficients and, hence, improves the robustness of the calibration model. Both kernel PLS and LS-SVM require the tuning of a parameter involved in the kernel function, but LS-SVM also requires the tuning of Γ (Coen et al., 2007). While both methods have their merits, non-linear kernel PLS is a logical extension of ordinary PLS and, hence, easier to understand for spectroscopists already familiar with PLS.

Nicolaï et al. (2006a) compared kernel PLS calibration models to ordinary PLS models for predicting the soluble solids content of apple. No significant difference in accuracy between kernel PLS and ordinary PLS calibration models was obtained, irrespective of the kernel and the applied transformation (none, log(1/R), Kubelka–Munck) or first order derivative calculation. Chauchard et al. (2004) found an improvement in the accuracy of LS-SVM calibration models for acidity of grapes compared to PLS and MLR but only when the LS-SVM model was implemented using scores of the spectra with respect to PLS latent variables. So far there does not seem to be convincing evidence that nonlinear techniques, such as ANNs or kernel-based methods can really offer advantages with respect to the classical linear algorithms. This is due to the fact that NIR spectroscopy is essentially a very linear technique. Further, Li et al. (1999) stated that both PCR and PLS can provide linear approximations to subtle deviations from ideal linear behaviour by using extra latent variables to account for the nonlinearity.

3.4. Outlier detection

Outliers may be induced by typing errors, file transfer, interface errors, sensor malfunctions and fouling, poor sensor calibration, bad sampling or sample presentation, etc. A sample may be outlying according to the X-variables only, to the Y-variables only, or to both. It may also not be an outlier for either separate sets of variables, but become an outlier when the X–Y relationship is considered.

In the calibration phase, outliers in the X-variables (spectra) show up in the PCA scores plot as points outside the normal range of variability. Alternatively, the leverage of a spectrum may be calculated as the distance to the centre of all spectra relative to the variability in its particular direction. If the leverage exceeds a certain threshold value (Velleman and Welsch, 1981), the spectrum may be considered as an outlier. Also, X-residuals plots can be constructed. Y-Outliers can be identified as extreme values in the Y-residuals plot. In practice, however, only those outliers which have an effect on the regression model are to be removed. Cook's influence measure is a combination of the leverage and the Y-residual and is usually plotted versus the observation number; large values indicate outliers which have a large influence on the calibration model (Næs et al., 2004). Excessive pruning of the data set for outliers should be avoided (Martens and Næs, 1998).

When the calibration model is implemented in a practical application, such as a sorting line, obviously only X-outliers can be identified. The leverage with respect to the calibration spectra may be compared to a threshold value. Also, it is directly related to the Hotelling T^2 statistic (Velleman and Welsch, 1981) – for

a sufficiently large number of observations, such as in a typical NIR calibration they can be considered equal – of which the distribution is known (Montgomery, 2005). If the Hotelling T^2 statistic is larger than some upper limit, the spectrum is classified as an outlier. Little attention has been paid in the literature to online detection of outliers, and more research is certainly required.

In order to assess the accuracy of the calibration model and to avoid overfitting, validation procedures have to be applied; a calibration model without validation is nonsense. *Leverage correction* is an equation based procedure to estimate the prediction accuracy without performing any prediction, and is to be avoided at all times because it always leads to overoptimistic estimates. In leave-one-out *cross validation*, one sample is removed from the dataset, and a calibration model is constructed for the remaining subset. The removed samples are then used to calculate the prediction residual. The process is repeated with other subsets until every sample has been left out once, and in the end the variance of all prediction residuals is estimated. In multifold cross validation, a well-defined number of samples ('segment') are left out instead of one. In *internal validation*, the dataset is split into a calibration and a validation set. The calibration model is constructed using the calibration set, and the prediction residuals are then calculated by applying the calibration model to the validation set. In *external validation*, the validation dataset is independent, and is, for example, obtained from a different orchard or different season. Although leverage correction should not be used, it is still the default cross validation method in the widely used Unscrambler chemometrics software (http://www.camo.com).

3.5. Model accuracy

The prediction error of a calibration model is defined as the root mean square error for cross validation (RMSECV) when cross validation is used or the root mean square error for prediction (RMSEP) when internal or external validation is used (Næs et al., 2004).

$$\text{RMSECV or RMSEP} = \sqrt{\frac{\sum_{i=1}^{n_p}(\hat{y}_i - y_i)^2}{n_p}}$$

with n_p the number of validated objects, and $\hat{y}_i$ and y_i the predicted and measured value of the ith observation in the test set, respectively. This value gives the average uncertainty that can be expected for predictions of future samples. The results of future predictions with a 95% confidence interval can be expressed as the predicted value $y_i \pm 1.96 \times \text{RMSEP}$. The number of latent variables in the calibration model is typically determined as that which minimises the RMSECV or RMSEP. In some publications the standard error of prediction (SEP) is reported instead of the RMSEP:

$$\text{SEP} = \sqrt{\frac{\sum_{i=1}^{n_p}(\hat{y}_i - y_i - b)^2}{n_p}}$$

with b the model bias. The RPD is defined as the ratio of the standard deviation of the response variable to the RMSEP or

RMSECV (some authors use the term SDR). An RPD between 1.5 and 2 means that the model can discriminate low from high values of the response variable; a value between 2 and 2.5 indicates that coarse quantitative predictions are possible, and a value between 2.5 and 3 or above corresponds to good and excellent prediction accuracy, respectively.

Another useful statistic is the R^2 value. It essentially represents the proportion of explained variance of the response variable in de calibration (R_c^2) or validation (R_v^2) set.

3.6. Model robustness

Calibration models are called robust when the prediction accuracy is relatively insensitive towards unknown changes of external factors. The main factors which may affect model performance are (Wang et al., 1991): (i) the calibration model developed on one instrument is transported to another instrument that produces instrumental responses that differ from the responses obtained on the first instrument; (ii) the instrumental responses measured on a single instrument drift because of temperature fluctuations, electronic drift, and changes in wavelength or detector stability over time; and (iii) the samples belong to different batches. The latter factor is in the case of NIR spectroscopy of fruit and vegetables probably the most important one, as the fruit matrix may be subject to within-tree variability (tree age, crop load, spur age, position within the tree and light effects), within-orchard variability (location of tree and light effects), orchard variability (soil characteristics, nutrition and weather conditions), fruit age and seasonal variability (Peirs et al., 2002b).

To illustrate the importance of model robustness, in Fig. 3 measured versus predicted values of the soluble solids content (%Brix) of Jonagold apple of two different orchards ('Orchard 1' and 'Orchard 2') and two seasons (2003 and 2004) are shown. Experimental conditions were as described in Nicolaï et al. (2006a). The spectral dataset obtained in 2003 from Orchard 1 was used to construct the calibration models using multifold cross validation with a segment size of 10 using a PLS algorithm implemented in Matlab 7.2 (The Mathworks, Natick, USA). Except for Fig. 3d the number of LVs was selected as the one minimising the RMSECV. In Fig. 3a, the 2003 dataset obtained from Orchard 1 was randomly split into a calibration and validation set (internal validation), leading to a RMSEP of 0.52% Brix which is close to the RMSECV (0.48% Brix). When the spectral data from the same orchard but different season (2004) are used for validation (Fig. 3b) the RMSEP increases to 0.89% Brix, while it further increases to 0.97% Brix (Fig. 3c) when data from both a different orchard (Orchard 2) and season (2). Interestingly enough, when the model complexity is reduced to 7 instead of 14 LVs, the RMSEP for the data from this different orchard and season decreases again to 0.68% Brix while the RMSECV increases to 0.51% Brix. Clearly model robustness increases at the expense of model accuracy.

While this example clearly shows that appropriate external validation is of prime importance for the successful application of multivariate calibration models, robustness issues have
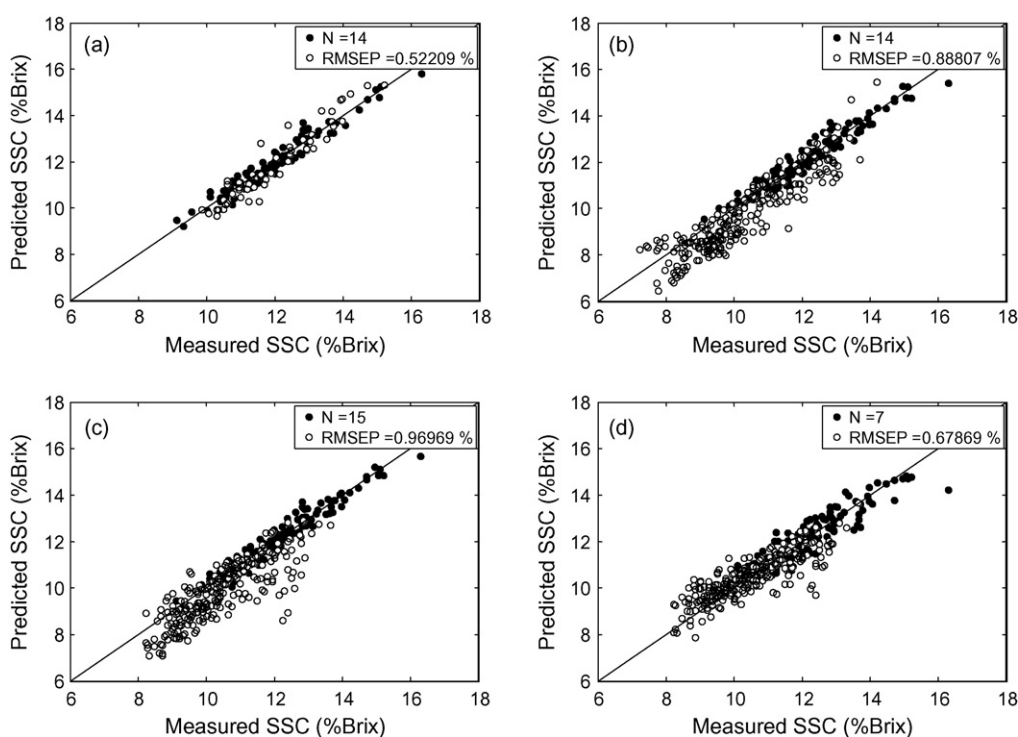
Fig. 3. Measured vs. predicted values of the soluble solids content (%Brix) of Jonagold apple based on NIR reflectance spectra. The calibration data were obtained in 2003 from Orchard 1. (a) Random division of dataset into calibration and (internal) validation set; (b) validation data from Orchard 1 in 2004; (c) validation data from Orchard 2 in 2004; (d) same as (c) but 7 instead of 14 LVs to increase model robustness at the expense of the RMSECV. The calibration and validation data are denoted by filled and empty circles, respectively.

received very little attention in the literature so far. Most calibration examples described in the literature were validated with measurements originating from the same sample batches as the calibration data set and it remains to be proven that the models are still valid for different batches. Only a few examples are available in which robustness has been considered. Lovász et al. (1994) evaluated the accuracy of a calibration model for dry matter of apple developed for one season on another season. Guthrie et al. (1998) found, based on calibrations for the SSC of pineapple and melon, a lack of robustness of calibration when fruit were harvested at different times. McGlone and Kawano (1998) collected kiwifruit of different sizes, different origins and different ages and stored them under varying conditions. When variability in origin, size and firmness were not considered in the calibration set, significantly higher validation errors were obtained. Similar results were found by Peirs et al. (2002b) for apple, Guthrie et al. (2005b) for mandarin, Guthrie et al. (2006) for rockmelon, and Golic and Walsh (2006) for peach and nectarine. In general the model error may easily double when a calibration model is applied to a spectral dataset of a different season or orchard. Also, lack of robustness often translates into bias. It is clear that in order to obtain a sufficiently robust calibration model, the calibration dataset should be sufficiently rich in variation and contain multiple orchards and seasons. Model robustness is the single most important concern in NIR spectroscopy of horticultural produce.

3.7. Calibration transfer

Spectrophotometers can vary both in wavelength calibration and photometric response. This is due to manufacturing tolerances, differences in optics, detectors and light sources, changes over time in the instrumental response function (ageing of sources, replacement of some parts, etc.), changes in the environment of the instrument over time (temperature, humidity) (Greensill et al., 2001; Fearn, 2001). As a consequence, calibration models developed for one spectrophotometer are as such useless on another device, even within one model. Commercial implementations of NIR spectroscopy in fruit or vegetable grading require the transferability of the calibration models from one spectrophotometer to another to avoid expensive repetition of the calibration procedure. This is certainly important for NIR spectroscopy of fruit and vegetables because of the large datasets required for robustness purposes.

Different calibration transfer techniques (also known as instrumental standardisation) have been developed over the past years to transfer a calibration model developed on a *master* (or *primary*) instrument to another instrument (*slave* or *secondary*). Essentially, spectra on the slave instruments are transformed so as to appear as if originating from the master instrument; the original calibration can then be used on the transformed spectra and no new calibration is required. It is also possible to transform the master spectra to appear as if originating from the slave instrument; new spectra may be added to the model in time but a calibration model must be developed for each slave instrument. Greensill et al. (2001) compared an array of techniques for calibration transfer between diode array systems, including

piecewise direct standardisation (PDS), orthogonal signal correction, the finite impulse response technique, model updating and a wavelet transform-based standardisation technique (WT). The best results were obtained with WT and model updating with RMSEPs of around 0.6–0.7% Brix for the SSC of melon with spectra measured on the slave instrument. The same authors obtained similar results for the SSC of mandarin with RMSEPs of around 0.3% Brix (Greensill and Walsh, 2002). Alamar et al. (2007) applied the PDS algorithm for calibration transfer between a diode array and a FT-NIR system as well as between two diode array systems of the same model for predicting SSC of apple. They obtained a RMSEP of around 0.7% Brix after PDS. We believe that model updating techniques are the method of choice—it seems natural to build in a procedure to constantly improve and adapt the accuracy of the calibrations with fresh samples.

3.8. Temperature effects

Temperature has a considerable effect on the NIR spectrum of chemical components. For example, the hydroxyl group of pure water causes a broad absorption band around 1449 nm due to a combination of antisymmetric and symmetric stretching modes of water (Maeda et al., 1995). This band is actually an overlay of at least five component spectra corresponding to water clusters with no, one, two, three and four hydrogen bonds. Raising the temperature decreases the average cluster size and increases the relative absorbance of the clusters with no hydrogen bonds causing a sharpening and shift of the hydroxyl band to lower wavelengths. Similar effects have been observed for NH stretching modes (Wülfert et al., 1998). In fruit and vegetable applications, temperature differences between calibration and validation set mainly cause bias (Golic and Walsh, 2006). Peirs et al. (2003a) found a bias of up to 0.3% Brix/°C when the soluble solids content of apple was 10% Brix, while Roger et al. (2003) found a bias of 0.4% Brix/°C for apple.

There are several methods to compensate for temperature fluctuations. Kawano et al. (1995) developed calibration equations using samples at different temperatures. Peirs et al. (2003a) proposed to either develop a global robust calibration model to cover the temperature range expected in future measurements, or to develop different models for dedicated temperatures. The first approach was followed with good result by Golic and Walsh (2006). Peirs et al. (2003a) also obtained good results when either the temperature was measured and included in $\mathbf{X}$ or simultaneously with the soluble solids content estimated from $\mathbf{X}$ using PLS2. A two-step PLS procedure in which first a calibration model was constructed for temperature using one LV only, and the calibration model for SSC was subsequently constructed based on the residual matrix gave poor results. In contrast, Roger et al. (2003) virtually removed the temperature induced bias in SSC by applying the external parameter orthogonalisation (EPO) algorithm as a preprocessing technique to remove that part from the spectral data matrix which is most affected by temperature. Similar results were obtained by Chauchard et al. (2004). More research is required to evaluate these techniques in different applications.

Table 1
Overview of applications of NIR spectroscopy to measure SSC of horticultural products

Species	Cultivar	Spectrophotometer	Acquisition mode	Spectral range	RMSEP	Ref.
Apple (*Malus domestica* Borkh.)	Jonagold	Scanning	Reflectance	380–1650	0.6 (SEP)	Lammertyn et al. (1998)
	Golden Delicious, Jonagold	PDA	Interactance	350–999	~1.1	Ventura et al. (1998)
	Empire, Golden and Red Delicious	Scanning	Reflectance	800–1700	0.4–0.5	Lu et al. (2000)
	Various	Scanning	Reflectance	380–2000	0.7	Peirs et al. (2000)
	Various	FT-NIR, scanning	Reflectance	1000–2000	0.7–0.9 (SEP)	Peirs et al. (2002a)
	Royal Gala	PDA	Interactance	500–1100	0.5–0.7	McGlone et al. (2002a)
	Various	PDA	Reflectance	800–1000	0.2 (SEP)	Temma et al. (2002a)
	Various	Scanning (?)	Reflectance	680–1235	0.3–0.5 (SEP)	Temma et al. (2002b)
	Royal Gala	PDA	Interactance	800–1000	0.3–0.5	McGlone et al. (2003a,b)
	Various	Scanning	Reflectance	380–2000	0.8–1.6	Peirs et al. (2003a,b)
		PDA	Interactance	300–1100	0.3	Walsh et al. (2004)
	Fuji	FT–NIR	Interactance	812–2357	0.5	Liu and Ying (2005)
	Golden Delicious	PDA	Reflectance	800–1690	0.4	Nicolaï et al. (2006a)
Apricot (*Prunus armeniaca* L.)	Boccuccia Sinosa, Errani	Scanning	Interactance	600–2500	0.9	Carlini et al. (2000)
Cherry (*Prunus serotina* L.)	Ravenna	Scanning	Interactance	600–2500	0.5	Carlini et al. (2000)
	Hedelfinger, Sam	Scanning	Reflectance	800–1700	0.7 (SEP)	Lu (2001)
Citrus fruit (*Citrus × limon* (L.) Burm.f.)	Jeju	PDA	Transmittance	636–1236	0.4 (SEP)	Lee et al. (2004)
Grape (*Vitis vinifera* L)	Cabernet Sauvignon, Carménère, Chardonnay	PDA	Transmittance/ Interactance	650–1100	1.1	Herrera et al. (2003)
Guava (*Psidium guajava* L.)	Pearl	Scanning	Reflectance	400–2498	0.8 (SEP)	Hsieh and Lee (2005)
Kiwifruit (*Actinidia chinensis* Planch)		PDA	Various	300–1100	0.8–1.2 (SEP)	Schaare and Fraser (2000)
Kiwifruit (*Actinidia deliciosa* (A. Chev.) C.F. Liang et A.R. Ferguson)	Hayward	PDA	Interactance	300–1140	0.5	McGlone et al. (2002b)
	Hayward	Scanning	Interactance	800–1100	0.4	McGlone and Kawano (1998)
Mandarin (*Citrus reticulata* L.)	Satsuma	Scanning	Transmittance	680–1235	0.3	Kawano et al. (1993)
	Imperial	PDA	Interactance	~730–930	0.2–0.4	Greensill and Walsh (2002)
	Satsuma Miyagawa	PDA	Various	700–930	0.3	McGlone et al. (2003a,b)
	?	PDA	Interactance	300–1100	0.5	Walsh et al. (2004)
	Imperial	PDA	Interactance	720–950	0.3–0.7	Guthrie et al. (2005a,b)
	Satsuma	Scanning	Reflectance	350–2500	0.3	Gómez et al. (2006)
Mango (*Mangifera indica* L.)	Tommy Atkins	Scanning	Reflectance	1200–2400	1.2	Schmilovitch et al. (2000)
	Caraboa	Scanning	Reflectance	1100–2500	0.7	Saranwong et al. (2001)

Table 1 (*Continued*)

Species	Cultivar	Spectrophotometer	Acquisition mode	Spectral range	RMSEP	Ref.
	Caraboa	Scanning, PDA	Interactance	400–1000; 600–1000	0.6–0.4	Saranwong et al. (2003a,b)
Melon (*Cucumis melo* L.)	Eldorado, Eastern Star, Hammersley	Scanning	Reflectance	700–1100	0.7–1.32 (SEP)	Guthrie et al. (1998)
	Doubloon, Navajo)	PDA	Interactance	630–1030	0.7–1.3	Greensill et al. (2001)
	Various	PDA	Interactance	306–1130	1	Guthrie et al. (2006)
	Eldorado, Eastern Star	PDA	Interactance	300–1150	0.4	Long and Walsh (2006)
Nectarine (*Prunus persica* (L.) Batsch)	Summerbrite	PDA	Interactance	735–932	0.8	Golic and Walsh (2006)
Papaya (*Carica papaya* L.)	Kapoho Solo	Scanning	Interactance	700–1100	1.1	Slaughter et al. (1999)
Peach (*Prunus persica* (L.) Batsch)	Shimizu Hakuto	Scanning	Interactance	680–1235	0.5	Kawano et al. (1992)
	Several	Scanning	Interactance	400–1100	0.6	Slaughter (1995)
	Nectarin	Scanning	Interactance	400–1100	0.6	Slaughter (1995)
		PDA	Interactance	300–1100	0.5	Walsh et al. (2004)
	Nectarin	PDA	Interactance	300–1100	0.3	Walsh et al. (2004)
	Honey, Sweet	FT–NIR	Interactance	800–2500	0.5	Ying et al. (2005)
	O'Henry	PDA	Interactance	735–932	0.8	Golic and Walsh (2006)
Pear (*Pyrus communis* L.)	Conference	NIR	Reflectance	780–1700	0.4	Nicolaï et al. (2007)
Pineapple (*Ananas comosus* (L.) Merill)	Smooth Cayenne	Scanning	Reflectance	400–2500	1.2 (SEP)	Guthrie and Walsh (1997)
	Smooth Cayenne	Scanning	Reflectance	700–1100	1.84 (SEP)	Guthrie et al. (1998)
Plum (*Prunus*)	Various	PDA	Interactance	306–1150	0.5–0.7	Golic and Walsh (2006)
	Autumn Giant	PDA	Interactance	735–932	0.8	Golic and Walsh (2006)

4. Applications

In Table 1, an overview is given of applications of NIR spectroscopy to measure the SSC of fruits and vegetables. Papers in conference proceedings have not been included to keep the list manageable. Only literature references in which at least an internal validation has been carried out have been included. Preprocessing techniques are not included because often a combination of various techniques is used. When the SEP and bias were reported they were converted to RMSEP ($RMSEP^2 = SEP^2 + bias^2$); when only the SEP was reported this was indicated in the table. Not surprisingly, most research has been carried out on apples, and only a few reports are on vegetables. A typical RMSEP seems to be around 0.5% Brix, but in the few applications where external validation sets from different orchards or seasons were used to calculate the RMSEP it is considerably higher (1–1.5% Brix). It is, therefore, likely that the RMSEP in the majority of publications is an underestimation of the error which is achievable in practical applications, such as grading lines. From Table 1 the feasibility of NIR spectroscopy to measure SSC in a wide variety of fruit is clear, and further progress can only be made when large datasets, encompassing several orchards and seasons and possibly fluctuating environmental conditions are considered.

Other applications of NIR spectroscopy of fruit and vegetables are shown in Table 2. While good calibration models were obtained for dry matter, it seems more difficult to predict acidity based on the NIR spectrum. The concentration of acids in most fruit and vegetables is typically considerably smaller than that of sugars, and probably too small to affect the NIR spectrum significantly. The water absorption bands dominate the spectrum of fruit and vegetables, and it is not likely that minor constituents can be measured well. Obviously, when the concentration of such a minor constituent is correlated to, e.g., sugar content, the calibration results may seem reasonable but then the method is indirect and robustness issues are to be expected when applied to a different batch.

Reasonable results have been obtained for texture attributes which are believed to be related to the scattering properties of the tissue. Multi- and hyperspectral techniques have been used to specifically address scattering and, hence, texture attributes (Table 3), and it is to be expected that more progress will be made by combining such techniques with more mechanistic light transport models. Also fruit maturity which is related to

Table 2
Overview of other applications of NIR spectroscopy in postharvest technology of fruits and vegetables

Species	Cultivar	Spectrophotometer	Acquisition mode	Spectral range (nm)	Attribute(s)	Reference
Apple (*Malus domestica* Borkh.)	Various	Scanning	Transmittance	800–1100	Firmness, pH, acidity, dry matter, alcohol insoluble solids	Lovász et al. (1994)
	Jonagold	Scanning	Reflectance	380–1650	Stiffness, pH	Lammertyn et al. (1998)
	Fuji	Scanning		1100–2500	Sugars	Cho et al. (1998)
	Various	Scanning	Reflectance	380–2000	Optimal harvest date, Streif index	Peirs et al. (2001)
	Royal Gala	PDA	Interactance	500–1100	Background colour, starch pattern index, firmness, quantitative starch, acidity	McGlone et al. (2002a)
	Various	FT–NIR, scanning	Reflectance	1000–2000	Firmness, acidity	Peirs et al. (2002a)
	Braeburn	PDA	Transmittance	300–1140	Brownheart disorder	Clark et al. (2003a,b)
	Royal Gala	PDA	Interactance	800–1000	Dry matter	McGlone et al. (2003a,b)
	Golden Delicious, Gala	Scanning	Reflectance	400–2498	Firmness	Park et al. (2003)
	Braeburn	PDA	Transmittance	650–950	Dry matter	McGlone and Martinsen (2004)
	Golden, Braeburn, Fuji	Scanning	Reflectance	400–2500	Sensory attributes	Mehinagic et al. (2004)
	Fuji	FT–NIR	Interactance	812–2357	Acidity, pH	Liu and Ying (2005)
	Braeburn	PDA	Transmittance	650–950	Brownheart disorder	McGlone et al. (2005)
	Various	Scanning	Reflectance	380–2000	Optimal harvest date	Peirs et al. (2005)
	Fuji	FT–NIR	Interactance	812–2357	Sugars	Liu et al. (2006)
	Golden Delicious	PDA	Reflectance	400–1700	Bruises	Xing et al. (2006)
Avocado (*Persea americana* Mill.)	Hass	PDA	Reflectance/ Interactance	300–1140	Dry matter	Clark et al. (2003a,b)
Banana (*Musa acuminata* Colla)	AAA group, Cavendish subgroup	Scanning	Reflectance	400–2500	Sugars	Tarkosova and Copikova (2000)
Caraway (*Carum carvi* L.)		Scanning	Reflectance	1108–2490	Essential oil content and composition	Schulz et al. (1998)
Coriander (*Coriandrum sativum* L.)		Scanning	Reflectance	1108–2490	Essential oil content and composition	Schulz et al. (1998)
Carrot (*Daucus carota* L.)	Various	FTIR	Reflectance	833–2500	Sugars, carotenoids	Schulz et al. (1998)
Chinese bayberry (*Myrica rubra* Siebold and Zuccarini)	Various	?	Reflectance	325–1075	Acidity	Li and He (2006)
Citrus fruit (*Citrus × limon* (L.) Burm.f.)	Unshiu	PDA	Transmittance	650–955	Defects, maturity	Kim et al. (2004)
Dill (*Anethum graveolens* L.)		Scanning	Reflectance	1108–2490	Essential oil content and composition	Schulz et al. (1998)
Fennel (*Foeniculum vulgare* Miller)		Scanning	Reflectance	1108–2490	Essential oil content and composition	Schulz et al. (1998)
		Scanning	Reflectance	1100–2498	Volatiles	Steuer and Shulz (2003)
Grape (*Vitis vinifera* L)	Merlot, Shiraz, Cabernet Sauvignon	PDA	Reflectance	400–1100	Colour, pH	Cozzolino et al. (2004)
Green beans (*Phaseolus vulgaris* L.)		FTIR	Reflectance	1000–2500	Cell wall pectins	Boeriu et al. (1998)
Guava (*Psidium guajava* L.)	Pearl	Scanning	Reflectance	400–2498	Hardness	Hsieh and Lee (2005)
Japanese pear (*Pyrus serotina* Rehder)	Housui	Scanning	Interactance	1100–2500	Pectin constituents	Sirisomboon et al. (2007)

Table 2 (*Continued*)

Species	Cultivar	Spectrophotometer	Acquisition mode	Spectral range (nm)	Attribute(s)	Reference
Kiwifruit (*Actinidia chinensis* Planch)		PDA	Various	300–1100	Density, internal flesh colour	Schaare and Fraser (2000), Clark et al. (2004)
Kiwifruit (*Actinidia deliciosa* (A. Chev.) C.F. Liang et A.R. Ferguson)	Hayward	Scanning	Interactance	800–1100	Firmness, dry matter	McGlone and Kawano (1998)
	Hayward	PDA	Interactance	300–1140	Dry matter	Osborne and Künnemeyer (1999)
	Hayward	PDA	Interactance	300–1140	Dry matter	McGlone et al. (2002b)
Macadamia (*Macadamia* F. Muell.*)*		Various	Various	Various	Quality defects	Guthrie et al. (2004)
Mandarin (*Citrus reticulata* L.)	Satsuma	Scanning	Transmittance	700-1000	Citric acid	Miyamoto et al. (1998)
	Satsuma Miyagawa	PDA	Various	700–930	Acidity	McGlone et al. (2003a,b)
	Imperial	PDA	Interactance	720–950	Dry matter	Guthrie et al. (2005a,b)
	Satsuma	Scanning?	Reflectance	350–2500	pH, firmness	Gómez et al. (2006)
Mango (*Magnifera indica* L.)		Scanning	Reflectance	400–2500	Dry matter	Guthrie and Walsh (1997)
	Tommy Atkins	Scanning	Reflectance	1200–2400	Acidity, firmness, storage period	Schmilovitch et al. (2000)
	Caraboa	Scanning	Reflectance	1100–2500	Dry matter	Saranwong et al. (2001)
	Mahajanaca	PDA	Interactance	600–1000	Dry matter, starch content	Saranwong et al. (2003b)
	Caraboa	Scanning	Interactance	700–1100	Dry matter, starch	Saranwong et al. (2004)
Melon (*Cucumis melo* L.)	Various	PDA	Interactance	306–1130	Dry matter	Guthrie et al. (2005a,b)
Mushroom (*Agaricus bisporus* (Lge.) Sing)		Scanning	Reflectance	400–2498	Moisture content	Roy et al. (1993)
Nectarine (*Prunus persica* (L.) Batsch)	Summerbrite	PDA	Interactance	735–932	Fresh weight	Golic and Walsh (2006)
Olive (*Olea europaea* L.)	Various	PDA	Reflectance	400–1700	Oil, moisture, oleic acid, linoleic acid	León et al. (2004)
	Various	FT	Reflectance	1010–2440	Quality disorders	Ayora-Cañada et al. (2005)
Onion (*Allium cepa* L.)	Southport White Globe, various	Scanning	Transmittance	700–1000	Dry matter	Birth et al. (1985)
Papaja (*Carica papaya* L.)		PDA	Transmittance	500–1000	Maturity	Greensill and Newman (1999)
Peach (*Prunus persica* (L.) Batsch)	Various	Scanning	Interactance	400–1100	Sugars, sweetness index, chlorophyll	Slaughter (1995)
	Nectarine	Scanning	Interactance	400–1100	Sugars, sweetness index, chlorophyll	Slaughter (1995)
		PDA	Transmittance	400–1000	Ripeness	Carlomagno et al. (2004)
	Honey, Sweet	FT–NIR	Interactance	800–2500	Available acid	Ying et al. (2005)
	Summerbrite	PDA	Interactance	735–932	Fresh weight	Golic and Walsh (2006)
Pear (*Pyrus communis* L.)	Conference	NIR	Reflectance	780–1700	Firmness	Nicolaï et al. (2007)
Pepper (*Piper nigrum* L.)		FT–NIR	Reflectance	833–2500	Oil constituents	Schulz et al. (2005a,b)

Table 2 (*Continued*)

Species	Cultivar	Spectrophotometer	Acquisition mode	Spectral range (nm)	Attribute(s)	Reference
Plum (*Prunus*)	Summerbrite	PDA	Interactance	735–932	Fresh weight	Golic and Walsh (2006)
Tangerine (*Citrus reticulata* L.)	Dancy	PDA	Transmittance	500–1000	Section drying disorder	Peiris et al. (1998)
Tomato (*Lycopersicon esculentum* L.)		PDA	Reflectance	500–1000	*Rhizopus stolonifer* spores	Hahn et al. (2004)
	House Momotaro	PDA	Interactance	305–1100	Dry matter	Khuriyati et al. (2004)
Yali pear (*Pyrus bretschneideri* Rehd.)	Yali	?	Transmittance	651-1282	Brown core	Han et al. (2006)

Table 3

Overview of multi- and hyperspectral imaging applications in postharvest technology of fruits and vegetables

Species	Cultivar	Optical setup	Spectral range	Application	Reference
Apple (*Malus domestica* Borkh.)	Red Delicious	CCD camera, combination with MIR camera	700–1000	Stem-Calyx identification	Wen and Tao (2000)
	Golden Delicious	CCD camera with imaging spectrograph, UV-A excitation for fluorescence imaging	430–930, selected wavelengths	Fecal contamination, bruises	Kim et al. (2001, 2002a,b)
	Jonagold	CCD camera with filters	450, 500, 750, 800	Surface defects	Kleynen et al. (2003, 2005)
	Red and Golden Delicious	InGaAs camera with imaging spectrograph	900–1700	Bruises	Lu (2003)
	Jonagold, Boskoop	InGaAs camera with imaging spectrograph	868–1789	Starch index	Peirs et al. (2003b)
	Various	CCD camera with imaging spectrograph.	424–899	Surface defects/contaminations	Mehl et al. (2004)
	Red Delicious	CCD with filter wheel	680, 880, 905, 940	Firmness	Lu (2004a)
	Red Delicious	CCD with filter wheel	680, 880, 905, 940, 1060	Firmness, SSC	Lu (2004b)
		InGaAs camera with imaging spectrograph	954–1350	Bitter pit	Nicolaï et al. (2006b)
	Honeycrisp, Redcort, Red Delicious	CCD with filter wheel	~450–940	Surface defects	Ariana et al. (2006a)
Cherry (*Prunus serotina* L.)		NIR camera with vidicon tube, monochromator controlled light source	680–1280	Defects	Guyer and Yang (2000)
Cherry (tart; *Prunus serotina* L.)	Montmorency	CCD with imaging spectrograph	450–1100	Pits	Qin and Lu (2005)
Cucumber (Cucumis sativus L.)		CCD camera with imaging spectrograph	447–951	Chilling injury	Cheng et al. (2004)
	Journey	InGaAs camera with imaging spectrograph	950–1650	Bruises	Ariana et al. (2006b)
Kiwifruit (*Actinidia deliciosa* (A. Chev.) C.F. Liang et A.R. Ferguson	Hayward	CCD camera with grating	650–1100	SSC distribution	Martinsen and Schaare (1998)
Melon (*Cucumis melo* L.)	Andes	CCD with band pass filter	676	SSC distribution	Sugiyama (1999)
		CCD with band pass filters	830, 850, 870, 905, 930	SSC distribution	Long et al. (2005)
Peach (*Prunus persica* (L.) Batsch)	Vesubio	CCD with band pass filters	830, 970	Bruises	Zwiggelaar et al. (1996)
	Red Haven, Coral Star	CCD with imaging spectrograph	500–1000	Firmness	Lu and Peng (2006)

both changes in sugar content and histology can be predicted well from NIR spectra. Other applications of multi- and hyperspectral techniques focussed on surface defects and the spatial distribution of the SSC in the fruit.

So far, most applications have been carried out in laboratory environments under static conditions. Notable exceptions addressing the problems with online implementations have been described by Steinmetz et al. (1999), Wen and Tao (2000), Cheng et al. (2003), Crowe and Delwiche (1996), McGlone and Martinsen (2004), Miller and Zude-Sasse (2004), McGlone et al. (2005) and Walsh et al. (2007). It appears that the industry is taking the lead in the development of online systems. The first grading line with a NIR sensor in reflectance mode was introduced in 1989 by Mitsui Minig Co., Ltd. (Japan) to sort peaches based on SSC (Kawano, 1998). Since then many manufacturers have followed, and grading lines equipped with NIR sensors are now commercially available from Aweta (IQA, http://www.aweta.nl), Greefa (iFA, http://www.greefa.nl), Mitsui-Kinzoku (http://www.mitsui-kinzoku.co.jp), Sacmi (F5, http://www.sacmi.it), TasteMark (http://www.taste-technologies.com), Color Vision Systems (Insight, http://www.cvs.com.au) and others. Unfortunately no scientific evidence is available about the accuracy of these systems.

5. Future research and conclusions

The feasibility of NIR spectroscopy to measure quality attributes of fruit and vegetables has now been shown for many products. The high acquisition speed of modern diode array based NIR spectrophotometers which often have an integration time well below 100 ms in combination with powerful multivariate calibration techniques, such as PLS, have finally brought online sorting of fruit and vegetables based on quality attributes rather than on external appearance within reach. The chances of a successful implementation depend on several factors, of which model robustness is the most important technical one. It is clear that the accuracy of the NIR calibration models should be sufficient even when they are used to predict quality attributes of product specimens which were not used in the model calibration. Calibration models to be used in practice should be based on large datasets, encompassing several orchards, climate conditions, seasons and operational conditions, such as temperature, and optimised towards robustness by incorporating appropriate preprocessing methods. Protocols are needed to update calibration models with minimal effort. Likewise, further research is necessary with respect to calibration techniques which rely on the actual physics of penetration of NIR radiation in fruit tissue rather than on a pure statistical analysis, such as PLS on empirically preprocessed spectra. Light transport simulations based on the diffusion approximation, the adding-doubling method or the Monte Carlo method might guide these research efforts, and make it possible to separate the information related to the physical (scattering) and chemical (absorption) properties of the biological tissue. Some very interesting preliminary results have been obtained recently (Fraser et al., 2003; Thennadil et al., 2006).

The availability of affordable hyperspectral cameras and spectrographs has provided exciting new possibilities for online defect detection which are not feasible with visible light. While acquisition speed is still an issue, focal plane array cameras may solve this problem. NIR microscopes implementing this technology have appeared recently, and it is expected that they will provide a better understanding of the microscopic distribution of, e.g., sugars or other interesting biochemical components at the histological or cellular level. Other interesting techniques which have not been sufficiently explored include space or time-resolved spectroscopy to separate absorption and scattering effects which may lead to novel and better calibration models for texture related attributes, and NIR Raman based techniques which only have been touched upon so far (e.g., Schrader et al., 1999; Schulz et al., 2005a,b).

To conclude, the most important factor for the success of online systems for grading of fruit and vegetables is the added commercial value which they can realise. Only when consumers are ready to pay premium prices for, e.g., extra sweet fruit, will auctions and packing houses be willing to purchase such grading lines and to change their quality system, which is now almost exclusively based on external appearance.

References

Alamar, M.C., Bobelyn, E., Lammertyn, J., Nicolaï, B.M., Moltó, E., 2007. Calibration transfer between NIR diode array and FT-NIR spectrophotometers for measuring the soluble solids content of apple. Postharvest Biol. Technol. 45, 38–45.

Ariana, D., Guyer, D.E., Shrestha, B., 2006a. Integrating multispectral reflectance and fluorescence imaging for defect detection on apples. Comp. Electron. Agric. 50, 148–161.

Ariana, D., Lu, R., Guyer, D.E., 2006b. Near-infrared hyperspectral reflectance imaging for detection of bruises on pickling cucumbers. Comp. Electron. Agric. 53, 60–70.

Ayora-Cañada, M.J., Muik, B., García-Mesa, J.A., Ortega-Calderón, D., Molina-Díaz, A., 2005. Fourier-transform near-infrared spectroscopy as a tool for olive fruit classification and quantitative analysis. Spectrosc. Lett. 38, 769–785.

Bearman, G., Levenson, R., 2001. Biological imaging spectroscopy. http://hdl.handle.net/2014/11729.

Bellon-Maurel, V., 1992. Application de la spectroscopie proche infrarouge au contrôle en ligne de la qualité des fruits et legumes. Thèse de doctorat. l'Institut National Polytechnique de Toulouse, France.

Birth, G.S., Dull, G.G., Renfroe, W.T., Kays, S.J., 1985. Nondestructive spectrophotometric determination of dry matter in onions. J. Am. Soc. Hortic. Sci. 110, 297–303.

Boeriu, C.G., Stolle-Smits, T., van Dijk, C., 1998. Characterisation of cell wall pectins by near infrared spectroscopy. J. Near Infrared Spectrosc. 6, A299–A301.

Carlini, P., Massantini, R., Mencarelli, F., 2000. Vis-NIR measurement of soluble solids in cherry and apricot by PLS regression and wavelength selection. J. Agric. Food Chem. 48, 5236–5242.

Carlomagno, G., Capozzo, L., Attolico, G., Distante, A., 2004. Non-destructive grading of peaches by near-infrared spectrometry. Infrared Phys. Technol. 46, 23–29.

Chauchard, F., Roger, J.M., Bellon-Maurel, V., 2004. Correction of the temperature effect on near infrared calibration—application to soluble solid content prediction. J. Near Infrared Spectrosc. 12, 199–205.

Cheng, X., Tao, Y., Chen, Y.R., Luo, Y., 2003. NIR/MIR dual-sensor machine vision system for online apple stem-end/calyx recognition. Trans. ASAE 46, 551–558.

Cheng, X., Chen, Y.R., Tao, C.Y., Wang, Y., Kim, M.S., Lefcourt, A.M., 2004. A novel integrated PCA and FLD method on hyperspectral image feature extraction for cucumber chilling damage inspection. Trans. ASAE 47, 1313–1320.

Cho, R.K., Sohn, M.R., Kwon, Y.K., 1998. New observation of nondestructive evaluation for sweetness in apple fruit using near infrared spectroscopy. J. Near Infrared Spectrosc. 6, A75–A78.

Clark, C.J., McGlone, V.A., De Silva, H.N., Manning, M.A., Burdon, J., Mowatt, A.D., 2004. Prediction of storage disorders of kiwifruit (*Actinidia chinensis*) based on visible-NIR spectral characteristics at harvest. Postharvest Biol. Technol. 32, 147–158.

Clark, C.J., McGlone, V.A., Jordan, R.B., 2003a. Detection of brownheart in 'Braeburn' apple by transmission NIR spectroscopy. Postharvest Biol. Technol. 28, 87–96.

Clark, C.J., McGlone, V.A., Requejo, C., White, A., Woolf, A.B., 2003b. Dry matter determination in 'Hass' avocado by NIR spectroscopy. Postharvest Biol. Technol. 29, 300–307.

Coen, T., Saeys, W., Ramon, H., De Baerdemaeker, J., 2007. Optimizing the tuning parameters of least squares support vector machines regression for NIR spectra. J. Chemom. 20, 184–192.

Cozzolino, D., Esler, M.B., Dambergs, R.G., Cynkar, W.U., Boehm, D.R., Francis, I.L., Gishen, M., 2004. Prediction of colour and pH in grapes using a diode array spectrophotometer (400–1100 nm). J. Near Infrared Spectrosc. 12, 105–111.

Cubeddu, R., Pfifferi, P., Taroni, P., Valentini, G., Torricelli, A., Valero, C., Ruiz-Altisent, M., Ortiz, C., 2001. Nondestructive quantification of chemical and physical properties of fruits by time-resolved reflectance spectroscopy in the wavelength range 650–1000 nm. Appl. Opt. 40, 538–543.

Crowe, T.G., Delwiche, M.J., 1996. Real-time defect detection in fruit. Part I. Design concepts and development of prototype hardware. Trans. ASAE 39, 2299–2308.

Davies, A.M., Grant, A., 1987. Review: near-infra-red analysis of food. Int. J. Food Sci. Technol. 22, 191–207.

Davies, A.M.C., 2000. William Herschel and the discovery of near infrared. Spectrosc. Eur. 12, 10–16.

De Belie, N., Tu, K., Jancsók, P., De Baerdemaeker, J., 1999. Preliminary study on the influence of turgor pressure on body reflectance of red laser light as a ripeness indicator for apples. Postharvest Biol. Technol. 16, 279–284.

Farrell, T.J., Patterson, M.S., 1992. A diffusion theory model of spatially resolved, steady-state diffuse reflectance for the non-invasive determination of tissue optical properties in vivo. Med. Phys. 19, 879–888.

Fearn, T., 2001. Standardisation and calibration transfer for near infrared instruments: a review. J. Near Infrared Spectrosc. 9, 229–244.

Fraser, D.G., Künnemeyer, R., McGlone, V.A., Jordan, R.B., 2000. Letter. Near infrared light penetration into an apple. Postharvest Biol. Technol. 22, 191–194.

Fraser, D.G., Jordan, R.B., Künnemeyer, R., McGlone, V.A., 2003. Light distribution inside mandarin fruit during internal quality assessment by NIR spectroscopy. Postharvest Biol. Technol. 27, 185–196.

Geladi, P., Dåbakk, E., 1995. An overview of chemometrics applications in near infrared spectrometry. J. Near Infrared Spectrosc. 3, 119–132.

Geladi, P., Martens, H., Hadjiiski, L., Hopke, P., 1996. A calibration tutorial for spectral data. Part 2. Partial least squares regression using Matlab and some neural network results. J. Near Infrared Spectrosc. 4, 243–255.

Golic, M., Walsh, K.B., 2006. Robustness of calibration models based on near infrared spectroscopy for the in-line grading of stonefruit for total soluble solids content. Anal. Chim. Acta 555, 286–291.

Gómez, H.A., He, Y., Pereira, A.G., 2006. Non-destructive measurement of acidity, soluble solids and firmness of Satsuma mandarin using Vis/NIR-spectroscopy techniques. J. Food Eng. 77, 313–319.

Greensill, C.V., Walsh, K.B., 2002. Calibration transfer between miniature photodiode array-based spectrometers in the near infrared assessment of mandarin soluble solids content. J. Near Infrared Spectrosc. 10, 27–35.

Greensill, C.V., Newman, D.S., 1999. An investigation into the determination of the maturity of pawpaws (*Carica papaya*) from NIR transmission spectra. J. Near Infrared Spectrosc. 7, 109–116.

Greensill, C.V., Walsh, K.B., 2000a. A remote acceptance probe and illumination configuration for spectral assessment of internal attributes of intact fruit. Meas. Sci. Technol. 11, 1674–1684.

Greensill, C.V., Walsh, K.B., 2000b. Optimisation of instrument precision and wavelength resolution for the performance of NIR calibrations of sucrose in a water-cellulose matrix. Appl. Spectrosc. 54, 426–430.

Greensill, C.V., Wolf, P.J., Spiegelman, C.H., Walsh, K.B., 2001. Calibration transfer between PDA-based NIR spectrometers in the NIR assessment of melon soluble solids content. Appl. Spectrosc. 55, 647–653.

Griffiths, P.R., 1995. Letter: practical consequences of math pre-treatment of near infrared reflectance data: log(1/R) vs. F(R). J. Near Infrared Spectrosc. 3, 60–62.

Gunasekaran, S., Irudayaraj, J., 2001. Optical methods: visible NIR and FTIR spectroscopy. In: Nondestructive Food Evaluation. Techniques to Analyse Properties and Quality. Marcel Dekker Inc., New York, USA.

Guthrie, J.A., Walsh, K.B., 1997. Non-invasive assessment of pineapple and mango fruit quality using near infra-red spectroscopy. Aust. J. Exp. Agric. 37, 253–263.

Guthrie, J.A., Wedding, B., Walsh, K.B, 1998. Robustness of NIR calibrations for soluble solids in intact melon and pineapple. J. Near Infrared Spectrosc. 6, 259–265.

Guthrie, J., Greensill, C., Bowden, R., Walsh, K., 2004. Assessment of quality defects in macadamia kernels using NIR spectroscopy. Aust. J. Agric. Res. 55, 471–476.

Guthrie, J.A., Walsh, K.B., Reid, D.J., Liebenberg, C.J., 2005a. Assessment of internal quality attributes of mandarin fruit I. NIR calibration model development. Aust. J. Agric. Res. 56, 405–416.

Guthrie, J.A., Reid, D.J., Walsh, K.B., 2005b. Assessment of internal quality attributes of mandarin fruit II. NIR calibration model robustness. Aust. J. Agric. Res. 56, 417–426.

Guthrie, J.A., Liebenberg, C.J., Walsh, K.B., 2006. NIR model development and robustness in prediction of melon fruit total soluble solids. Aust. J. Agric. Res. 57, 1–8.

Guyer, D., Yang, X., 2000. Use of genetic artificial neural networks and spectral imaging for defect detection on cherries. Comp. Electron. Agric. 29, 179–194.

Hahn, F., Lopez, I., Hernandez, G., 2004. Spectral detection and neural network discrimination of *Rhizopus stolonifer* spores on red tomatoes. Biosyst. Eng. 89, 93–99.

Han, D., Tu, R., Lu, C., Liu, C., Wen, Z., 2006. Nondestructive detection of brown core in the Chines pear 'Yali' by transmission visible-NIR spectroscopy. Food Control 17, 604–608.

Hernández Sánchez, N., Lurol, S., Roger, J.M., Bellon-Maurel, V., 2003. Robustness of models based on NIR spectra for sugar content prediction in apples. J. Near Infrared Spectrosc. 11, 97–107.

Herrera, J., Guesalaga, A., Agosin, E., 2003. Shortwave-near infrared spectroscopy for non-destructive determination of maturity of wine grapes. Meas. Sci. Technol. 14, 689–697.

Hsieh, C., Lee, Y., 2005. Applied visible/near-infrared spectroscopy on detecting the sugar content and hardness of pearl guava. Trans. ASAE 21, 1039–1046.

Il'yasov, S.G., Krasnikov, V.V., 1991. Physical Principals of Infrared Irradiation of Foodstuffs. Hemisphere Publishin Corporation, New York, USA.

Isaksson, T., Næs, T., 1988. The effect of multiplicative scatter correction and linearity improvement in NIR spectroscopy. Appl. Spectrosc. 42, 1273–1284.

Jacques, S.L., 1998. Light distributions from point, line and plane sources for photochemical reactions and fluorescence in turid biological tissues. Photochem. Photobiol. 67, 23–32.

Kawano, S., Abe, H., Iwamoto, M., 1995. Development of a calibration equation with temperature compensation for determining the Brix value in intact peaches. J. Near Infrared Spectrosc. 3, 211–218.

Kawano, S., Watanabe, H., Iwamoto, M., 1992. Determination of sugar content in intact peaches by near infrared spectroscopy with fiber optics in interactance mode. J. Jpn. Soc. Hortic. Sci. 61, 445–451.

Kawano, S., Fujiwara, T., Iwamoto, M., 1993. Nondestructive determination of sugar content in Satsuma mandarin using near infrared (NIR) transmittance. J. Jpn. Soc. Hortic. Sci. 62, 465–470.

Kawano, S., 1998. New application of nondestructive methods for quality evaluation of fruits and vegetables in Japan. J. Japan. Soc. Hort. Sci. 67, 1176–1179.

Khuriyati, N., Matsuoka, T., Kawano, S., 2004. Precise near infrared spectral acquisition of intact tomatoes in interactance mode. J. Near Infrared Spectrosc. 12, 391–395.

Kim, G., Lee, K., Choi, K., Son, J., Choi, D., Kang, S., 2004. Defect and ripeness inspection of citrus using NIR transmission spectrum. Key Eng. Mater. 270–273, 1008–1013.

Kim, J., Mowat, A., Poole, P., Kasabov, N., 2000. Linear and non-linear pattern recognition models for classification of fruit from visible-near infrared spectra. Chemom. Intell. Lab. Syst. 51, 201–216.

Kim, M.S., Chen, Y.R., Mehl, P.M., 2001. Hyperspectral reflectance and fluorescence imaging system for food quality and safety. Trans. ASAE 44, 721–729.

Kim, M.S., Lefcourt, A.M., Chao, K., Chen, Y.R., Kim, I., Chan, D.E., 2002a. Multispectral detection of fecal contamination on apples based on hyperspectral imagery. Part I. Application of visible and near-infrared reflectance imaging. Trans. ASAE 45, 2027–2037.

Kim, M.S., Lefcourt, A.M., Chen, Y.R., Kim, I., Chan, D.E., Chao, K., 2002b. Multispectral detection of fecal contamination on apples based on hyperspectral imagery Part II. Application of hyperspectral fluorescence imaging. Trans. ASAE 45, 2039–2047.

Kleynen, O., Leemans, V., Destain, M.-F., 2003. Selection of the most efficient wavelength bands for 'Jonagold' apple sorting. Postharvest Biol. Technol. 30, 221–232.

Kleynen, O., Leemans, V., Destain, M.-F., 2005. Development of a multi-spectral vision system for the detection of defects on apples. J. Food Eng. 69, 41–49.

Lammertyn, J., Nicolaï, B., Ooms, K., De Smedt, V., De Baerdemaeker, J., 1998. Non-destructive measurement of acidity, soluble solids, and firmness of Jonagold apples using NIR spectroscopy. Trans. ASAE 41, 1089–1094.

Lammertyn, J., Peirs, A., De Baerdemaeker, J., Nicolaï, B., 2000. Light penetration properties of NIR radiation in fruit with respect to non-destructive quality assessment. Postharvest Biol. Technol. 18, 121–132.

Lee, K., Kim, G., Kang, S., Son, J., Choi, D., Choi, K., 2004. Measurement of sugar content in citrus using near infrared transmittance. Key Eng. Mater. 270–273, 1014–1019.

León, L., Garrido-Varo, A., Downey, G., 2004. Parent and harvest year effects on near-infrared reflectance spectroscopic analysis of olive (*Olea europeana* L) fruit traits. J. Agric. Food Chem. 52, 4957–4962.

Li, Y., Brown, C.W., Lo, S., 1999. Near infrared spectroscopic determination of alcohols: solving non-linearity with linear and non-linear methods. J. Near Infrared Spectrosc. 7, 55–62.

Li, X., He, Y., 2006. Non-destructive measurement of acidity of Chinese bayberry using Vis/NIR techniques. Eur. Food Res. Technol. 223, 731–736.

Liu, Y., Ying, Y., 2005. Use of FT-NIR spectrometry in non-invasive measurements of internal quality of 'Fuji' apples. Postharvest Biol. Technol. 37, 65–71.

Liu, Y., Ying, Y., Yu, H., Fu, X., 2006. Comparison of the HPLC method and FT-NIR analysis for quantification of glucose, fructose and sucrose in intact apple fruits. J. Agric. Food Chem. 54, 2810–2815.

Long, R.L., Walsh, K.B., Greensill, C.V., 2005. Sugar 'imaging' of fruit using a low cost CCD camera. J. Near Infrared Spectrosc. 13, 177–186.

Long, R.L., Walsh, K.B., 2006. Limitations to the measurement of intact melon total soluble solids using near infrared spectroscopy. Aust. J. Agric. Res. 57, 403–410.

Lovász, T., Merész, P., Salgó, A., 1994. Application of near infrared transmission spectroscopy for the determination of some quality parameters of apples. J. Near Infrared Spectrosc. 2, 213–221.

Lu, R., Guyer, D.E., Beaudry, R.M., 2000. Determination of firmness and sugar content of apples using near-infrared diffuse reflectance. J. Text. Stud. 31, 615–630.

Lu, R., 2001. Predicting firmness and sugar content of sweet cherries using near-infrared diffuse reflectance spectroscopy. Trans. ASAE 44, 1265–1271.

Lu, R., 2003. Detection of bruises on apples using near-infrared hyperspectral imaging. Trans. ASAE 46, 523–530.

Lu, R., 2004a. Prediction of apple fruit firmness by near-infrared multispectral scattering. J. Text. Stud. 35, 263–276.

Lu, R., 2004b. Multispectral imaging for predicting firmness and soluble solids content of apple fruit. Postharvest Biol. Technol. 31, 147–157.

Lu, R., Peng, Y., 2006. Hyperspectral scattering for assessing peach fruit firmness. Biosyst. Eng. 93, 161–171.

Maeda, H., Ozaki, Y., Tanaka, M., Hayashi, N., Kojima, T., 1995. Near infrared spectroscopy and chemometrics studies of temperature dependent spectral variations of water: relationship between spectral changes and hydrogen bonds. J. Near Infrared Spectrosc. 3, 191–201.

Martens, H., Stark, E., 1991. Extended multiplicative signal correction and spectral interference subtraction—new preprocessing methods for near-infrared spectroscopy. J. Pharm. Biomed. Anal. 9, 625–635.

Martens, H., Næs, T., 1998. Multivariate Calibration. John Wiley & Sons Ltd., Chichester, Great Britain.

Martinsen, P., Schaare, P., 1998. Measuring soluble solids distribution in kiwifruit using near-infrared imaging spectroscopy. Postharvest Biol. Technol. 14, 271–281.

McGlone, V.A., Abe, H., Kawano, S., 1997. Kiwifruit firmness by near infrared light scattering. J. Near Infrared Spectrosc. 5, 83–89.

McGlone, V.A., Kawano, S., 1998. Firmness, dry-matter and soluble-solids assessment of postharvest kiwifruit by NIR-spectroscopy. Postharvest Biol. Technol. 13, 131–141.

McGlone, V.A., Jordan, R.B., Martinsen, P.J., 2002a. Vis/NIR estimation at harvest of pre- and post-storage quality indices for 'Royal Gala' apple. Postharvest Biol. Technol. 25, 135–144.

McGlone, V.A., Jordan, R.B., Seelye, R., Martinsen, P.J., 2002b. Comparing density and NIR methods for measurement of Kiwifruit dry matter and soluble solids content. Postharvest Biol. Technol. 26, 191–198.

McGlone, V.A., Fraser, D., Jordan, R.B., Künnemeyer, R., 2003a. Internal quality assessment of mandarin fruit by vis/NIR spectroscopy. J. Near Infrared Spectrosc. 11, 323–332.

McGlone, V.A., Jordan, R.B., Seelye, R., Clark, C.J., 2003b. Dry-matter—a better predictor of the post-storage soluble solids in apples? Postharvest Biol. Technol. 28, 431–435.

McGlone, V.A., Martinsen, P.J., 2004. Transmission measurements on intact apples moving at high speed. J. Near Infrared Spectrosc. 12, 37–43.

McGlone, V.A., Martinsen, P.J., Clark, C.J., Jordan, R.B., 2005. On-line detection of Brownheart in Braeburn apples using near infrared transmission measurements. Postharvest Biol. Technol. 37, 142–151.

Mehinagic, E., Royer, G., Symoneaux, R., Bertrand, D., Jourjon, F., 2004. Prediction of the sensory quality of apples by physical measurements. Postharvest Biol. Technol. 34, 257–269.

Mehl, P.M., Chen, Y.R., Kim, M., Chan, D.E., 2004. Development of a hyperspectral imaging system for the detection of apple surface defects and contaminations. J. Food Eng. 61, 67–81.

Miller, W.M., Zude-Sasse, M., 2004. NIR-based sensing to measure soluble solids content of florida citrus. Appl. Eng. Agric. 20, 321–327.

Miyamoto, K., Kawauchi, M., Fukuda, T., 1998. Classification of high acid fruits by partial least squares using the near infrared transmittance spectra of intact satsuma mandarins. J. Near Infrared Spectrosc. 6, 267–271.

Montgomery, D.C., 2005. Statistical Process Control. John Wiley and Sons, Inc.

Næs, T., Kvaal, K., Isaksson, T., Miller, C., 1993. Artificial neural networks in multivariate calibration. J. Near Infrared Spectrosc. 1, 1–11.

Næs, T., Isaksson, T., Fearn, T., Davies, T., 2004. A User-friendly Guide to Multivariate Calibration and Classification. NIR publications, Charlton, Chichester, UK.

Nicolaï, B.M., Theron, K.I., Lammertyn, J., 2006a. Kernel PLS regression on wavelet transformed NIR spectra for prediction of sugar content of apple. Chemom. Intell. Lab. Syst. 85, 243–252.

Nicolaï, B.M., Lötze, E., Peirs, A., Scheerlinck, N., Theron, K.I., 2006b. Non-destructive measurement of bitter pit in apple fruit using NIR hyperspectral imaging. Postharvest Biol. Technol. 40, 1–6.

Nicolaï, B.M., Verlinden, B.E., Desmet, M., Saevels, S., Theron, K., Cubeddu, R., Pifferi, A., Torricelli, A., 2007. Time-resolved and continuous wave NIR reflectance spectroscopy to predict firmness and soluble solids content of Conference pears. Postharvest Biol. Technol., doi:10.1016/j.postharvbio.2007.06.001, in press.

Oey, M.L., Vanstreels, E., De Baerdemaeker, J., Tijskens, E., Ramon, H., Hertog, M., Nicolaï, B.M., 2007. Effect of turgor on micromechanical and structural properties of apple tissue: a quantitative analysis. Postharvest Biol. Technol. 44, 240–247.

Norris, K.H., 1964. Design and development of a new moisture meter. Agric. Eng. 45, 370.

Osborne, S.D., Künnemeyer, R., 1999. A low-cost system for the grading of kiwifruit. J. Near Infrared Spectrosc. 7, 9–15.

Park, B., Abbott, J.A., Lee, K.J., Choi, C.H., Choi, K.H., 2003. Near-infrared diffuse reflectance for quantitative and qualitative measurement of soluble solids and firmness of Delicious and Gala apples. Trans. ASAE 46, 1721–1731.

Peiris, K.H.S., Dull, G.G., Leffler, R.G., Kays, S.J., 1999. Spatial variability of soluble solids or dry-matter content within individual fruits, bulbs, or tubers: implications for the development and use of NIR spectrometric techniques. HortScience 34, 114–118.

Peiris, K.H.S., Dull, G.G., Leffler, R.G., Burns, J.K., Thai, C.N., Kays, S.J., 1998. Nondestructive detection of section drying, and internal disorder in tangerine. HortScience 33, 310–312.

Peirs, A., Ooms, K., Lammertyn, J., Nicolaï, B., 2001. Prediction of the optimal picking date of different apple cultivars by means of VIS/NIR-spectroscopy. Postharvest Biol. Technol. 21, 189–199.

Peirs, A., Scheerlinck, N., Touchant, K., Nicolaï, B.M., 2002a. Comparison of Fourier transform and dispersive near infrared reflectance spectroscopy for apple quality measurements. Biosyst. Eng. 81 (3), 305–311.

Peirs, A., Tirry, J., Verlinden, B., Darius, P., Nicolaï, B.M., 2002b. Effect of biological variability on the robustness of NIR-models for soluble solids content of apples. Postharvest Biol. Technol. 28, 269–280.

Peirs, A., Scheerlinck, N., Nicolaï, B.M., 2003a. Temperature compensation for near infrared reflectance measurement of apple fruit soluble solids contents. Postharvest Biol. Technol. 30, 233–248.

Peirs, A., Scheerlinck, N., De Baerdemaeker, J., Nicolaï, B.M., 2003b. Starch index determination of apple fruit by means of a hyperspectral near infrared reflectance imaging system. J. Near Infrared Spectrosc. 11 (379–389), 2003.

Peirs, A., Schenk, A., Nicolaï, B.M., 2005. Effect of natural variability among apples on the accuracy of VIS-NIR calibration models for optimal harvest date predictions. Postharvest Biol. Technol. 35, 1–13.

Polessello, A., Giangiacomo, R., 1981. Application of near infrared spectrophotometry to the nondestructive analysis of foods: a review of experimental results. Crit. Rev. Food Sci. Nutr. 18, 203–230.

Prahl, S.A., 1995. The adding-doubling method. In: Welch, A.J., van Gemert, M.J.C. (Eds.), Optical Thermal Response of Laser Irradiated Tissue. Plenum Press, New York, pp. 101–129.

Qin, J., Lu, R., 2005. Detection of pits in tart cherries by hyperspectral transmission imaging. Trans. ASAE 48, 1700–1963.

Roger, J.-M., Chauchard, F., Bellon-Maurel, V., 2003. EPO-PLS external parameter orthogonalisation of PLS application to temperature-independent measurement of sugar content of intact fruits. Chemom. Intell. Lab. Syst. 66, 191–204.

Rosipal, R., Trejo, L.J., 2001. Kernel partial least squares regression in reproducing kernel Hilbert space. J. Mach. Learn. Res. 2, 97–123.

Roy, S., Anantheswaran, R., Shenk, J., Westerhaus, M.O., Beelman, R., 1993. Determination of moisture content of mushrooms by VIS-NIR-spectroscopy. J. Sci. Food Agric. 63, 355–360.

Saranwong, S., Sornsrivichai, J., Kawano, S., 2001. Improvement of PLS calibration for Brix value and dry matter of mango using information from MLR calibration. J. Near Infrared Spectrosc. 9, 287–295.

Saranwong, S., Sornsrivichai, J., Kawano, S., 2003b. On-tree evaluation of harvesting quality of mango fruit using a hand-held NIR instrument. J. Near Infrared Spectrosc. 11, 283–293.

Saranwong, S., Sornsrivichai, J., Kawano, S., 2003a. Performance of a portable near infrared instrument for Brix value determination of intact mango fruit. J. Near Infrared Spectrosc. 11, 175–181.

Saranwong, S., Sornsrivichai, J., Kawano, S., 2004. Prediction of ripe-stage eating quality of mango fruit from its harvest quality measured nondestructively by near-infrared spectroscopy. Postharvest Biol. Technol. 31, 137–145.

Schaare, P.N., Fraser, D.G., 2000. Comparison of reflectance, interactance and transmission modes of visible-near infrared spectroscopy for measuring internal properties of kiwifruit (*Actinidia chinensis*). Postharvest Biol. Technol. 20, 175–184.

Schmilovitch, Z., Mizrach, A., Hoffman, A., Egozi, H., Fuchs, Y., 2000. Determination of mango physiological indices by near-infrared spectrometry. Postharvest Biol. Technol. 19, 245–252.

Schrader, B., Dippel, B., Erb, I., Keller, S., Löchte, T., Schulz, H., Tatsch, E., Wessel, S., 1999. NIR Raman spectroscopy in medicine and biology: results and aspects. J. Mol. Struct. 480–481, 21–32.

Schulz, H., Baranska, M., Baranski, R., 2005a. Potential of NIR-FT-Raman spectroscopy in natural carotenoid analysis. Biopolymers 77, 212–221.

Schulz, H., Baranska, M., Quilitzsch, Schütze, W., Lösing, G., 2005b. Characterization of peppercorn, pepper oil, and pepper oleoresin by vibrational spectroscopy methods. J. Agric. Food Chem. 53, 3358–3363.

Schulz, H., Drews, H.H., Quilitzsch, R., Krüger, H., 1998. Application of near infrared spectroscopy for the quantification of quality parameters in selected vegetables and essential oil plants. J. Near Infrared Spectrosc. 6, A125–A130.

Sharpe, P.J.H., Barber, H.N., 1972. Near infrared reflectance of colored fruits. Appl. Opt. 11, 2902–2905.

Shawe-Taylor, J., Cristianini, N., 2004. Kernel Methods for Pattern Analysis. Cambridge University Press, Cambridge.

Sirisomboon, P., Tanaka, M., Fujita, S., Kojima, T., 2007. Evaluation of pectin constituents of Japanese pear by near infrared spectroscopy. J. Food Eng. 78, 701–707.

Slaughter, D., 1995. Non-destructive determination of internal quality in peaches and nectarines. Trans. ASAE 38, 617–623.

Slaughter, D.C., Cavaletto, C.G., Gautz, L.D., Paull, R.E., 1999. Non-destructive determination of soluble solids in papayas using near infrared spectroscopy. J. Near Infrared Spectrosc. 7, 223–228.

Steinmetz, V., Roger, J.M., Moltó, E., Blasco, J., 1999. On-line fusion of colour camera and spectrophotometer for sugar content prediction of apples. J. Agric. Eng. Res. 73, 207–216.

Steuer, B., Shulz, H., 2003. Near-infrared analysis of fennel (*Foeniculum vulgare* Miller) on different spectrometers – Basic considerations for a reliable network. Phytochem. Anal. 14, 285–289.

Stratis, D.N., Eland, K.L., Carter, J.C., Tomlinson, S.J., Angel, S.M., 2001. Comparison of acousto-optic and liquid crystal tunable filters for laser-induced breakdown spectroscopy. Appl. Spectrosc. 55, 999–1004.

Sugiyama, J., 1999. Visualization of sugar content in the flesh of a melon by near infrared imaging. J. Agric. Food Chem. 47, 2715–2718.

Tarkosova, J., Copikova, J., 2000. Determination of carbohydrate content in bananas during ripening and storage by near infrared spectroscopy. J. Near Infrared Spectrosc. 8, 21–26.

Temma, T., Hanamatsu, K., Shinoki, F., 2002a. Development of a portable near infrared sugar-measuring instrument. J. Near Infrared Spectrosc. 10, 77–83.

Temma, T., Hanamatsu, K., Shinoki, F., 2002b. Measuring the sugar content of apples and apple juice by near infrared spectroscopy. Opt. Rev. 9, 40–44.

Thennadil, S.N., Martens, H., Kohler, A., 2006. Physics-based multiplicative scatter correction approaches for improving the performance of calibration models. Appl. Spectrosc. 60, 315–321.

Tu, K., De Busscher, R., De Baerdemaeker, J., Schrevens, E., 1995. Using laser beam as light source to study tomato and apple quality non-destructively. In: Proceedings of the Food Processing Automation IV Conference, ASAE, Chicago, IL, pp. 528–536.

Tu, K., Jancsók, P., Nicolaï, B.M., De Baerdemaeker, J., 2000. Use of laser scattering imaging to study tomato fruit quality in relation to acoustic and compression measurements. Int. J. Food Sci. Technol. 35, 503–510.

Upchurch, B.L., Throop, J.A., 1994. Effects of storage duration on detecting watercore in apples using machine vision. Trans. ASAE 37, 483–486.

Valero, C., Ruiz-Altisent, M., Cubeddu, R., Pifferi, A., Taroni, P., Torricelli, A., Valentini, G., Johnson, D.S., Dover, C.J., 2004. Detection of internal quality in kiwi with time-domain diffuse reflectance spectroscopy. Appl. Eng. Agric. 20, 223–230.

Velleman, P.F., Welsch, R.E., 1981. Efficient computing of regression diagnostics. Am. Stat. 35, 234–242.

Ventura, M., De Jager, A., de PutterF H., RoelofsF F.P.M.M., 1998. Nondestructive determination of soluble solids in apple fruit by near infrared spectroscopy (NIRS). Postharvest Biol. Technol. 14, 21–27.

Walsh, K.B., Golic, M., Greensill, C.V., 2004. Sorting of fruit using near infrared spectroscopy: application to a range of fruit and vegetables for soluble solids and dry matter content. J. Near Infrared Spectrosc. 12, 141–148.

Walsh, K.B., Guthrie, J.A., Burney, J.W., 2000. Application of commercially available, low-cost, miniaturised NIR spectrometers to the assessment of the sugar content of intact fruit. Aust. J. Plant Physiol. 27, 1175–1186.

Walsh, K.B., Long, R.L., Middelton, S.G., 2007. Use of near infra-red spectroscopy in evaluation of source-sink manipulation to increase the soluble sugar content of stonefruit. J. Hortic. Sci. Biotechnol. 82, 316–322.

Wang, Y., Veltkamp, D.J., Kowalski, B.R., 1991. Multivariate instrument standardisation. Anal. Chem. 63, 2750–2756.

Wang, L.-H., Jacques, S.L., Zheng, L.-Q., 1995. MCML—Monte Carlo modeling of photon transport in multi-layered tissues. Comp. Meth. Prog. Biomed. 47, 131–146.

Wen, Z., Tao, Y., 2000. Dual-camera NIR/MIR imaging for stem-end/calyx identification in apple defect sorting. Trans. ASAE 43, 449–452.

Wold, S., Sjöström, M., Eriksson, L., 2001. PLS-regression: a basic tool of chemometrics. Chemom. Intell. Lab. Syst. 58, 109–130.

Wülfert, F., Kok, W.T., Smilde, A.K., 1998. Influence of temperature on vibrational spectra and consequences for the predictive ability of multivariate models. Anal. Chem. 70, 1761–1767.

Xing, J., Bravo, C., Moshou, D., Ramon, H., De Baerdemaeker, J., 2006. Bruise detection on 'Golden Delicious' apples by vis/NIR spectroscopy. Comp. Electron. Agric. 52, 11–20.

Ying, Y.B., Liu, Y.D., Wang, J.P., Fu, X.P., Li, Y.B., 2005. Fourier transform near-infrared determination of total soluble solids and available acid in intact peaches. Trans. ASAE 48, 229–234.

Zude, M., Herold, B., Roger, J.-M., Bellon-Maurel, V., Landahl, S., 2006. Nondestructive tests on the prediction of apple fruit flesh firmness and soluble solids content on tree and in shelf life. J. Food Eng. 77, 254–260.

Zwiggelaar, R., Yang, Q., Garcia-Pardo, E., Bull, C.R., 1996. Use of spectral information and machine vision for bruise detection on peaches and apricots. J. Agric. Eng. Res. 63, 323–332.